Performance and Reliability Improvement of Partially Shaded PV Arrays by One-Time Electrical Reconfiguration

PRIYA RANJAN SATPATHY[1], **PRITAM BHOWMIK**[2], **(Member, IEEE),**
THANIKANTI SUDHAKAR BABU[1], **(Senior Member, IEEE),**
CHIRANJIT SAIN[3], **(Member, IEEE), RENU SHARMA**[4], **(Senior Member, IEEE),**
AND HASSAN HAES ALHELOU[5], **(Senior Member, IEEE)**

[1]Department of Electrical and Electronics Engineering, Chaitanya Bharathi Institute of Technology, Hyderabad 500075, India
[2]Department of Electrical Engineering, Budge Budge Institute of Technology, Kolkata 700137, India
[3]Department of Electrical Engineering, Ghani Khan Choudhury Institute of Engineering & Technology, Malda, West Bengal 732141, India
[4]Department of Electrical Engineering, ITER, Siksha 'O' Anusandhan Deemed to be University, Bhubaneswar 751030, India
[5]Department of Electrical Power Engineering, Faculty of Mechanical and Electrical Engineering, Tishreen University, Lattakia 2230, Syria

Corresponding authors: Hassan Haes Alhelou (alhelou@ieee.org) and Thanikanti Sudhakar Babu (sudhakarbabu66@gmail.com)

ABSTRACT Partial shading is the most unexpected scenario encountered by the arrays that degrade the performance causing power reduction, non-convex characteristics curves, losses, hotspot, module damage, and system failure. The adoption of various reconfiguration techniques has recently provided relief to the PV array to reduce power losses during partial shading. However, these techniques exhibit vulnerabilities such as reliable operation, ease of implementation and, higher cost and complexity due to the requirement of abundant manpower, labour, complex algorithms, dynamic operation, switches and sensors that cause additional power losses. Hence, this paper presents a low cost and less complex reconfiguration technique for PV arrays to effectively increase the power generation during partial shading scenarios. The proposed reconfiguration does not require any manpower, labour, algorithms or additional devices to reduce the losses in arrays during shading. The efficacy of the technique is tested using two array sizes under various shading scenarios using MATLAB modelling and real-time field experiments. Also, for better analysis, the performance of the proposed technique is compared with conventional configurations and Sudoku reconfiguration. The investigation proclaimed that the proposed reconfiguration technique has an average power enhancement of 20% higher than any other conventional configurations.

INDEX TERMS Photovoltaic (PV), partial shading, mismatch loss, multiple peaks, power generation.

I. INTRODUCTION

Solar Photovoltaic (PV) is one of the fastest-growing and adopted energy generation sources that utilize the energy of the sun to generate electrical energy [1]. Besides being a renewable energy source, the solar PV system exhibits various other supremacy of being a reliable and noise-less generating source. However, the system encounters a major demerit of partial shading that causes severe losses and complexities while generating the maximum power equivalent to the irradiance and operating temperature [2].

Partial shading mainly occurs due to various factors that include shadows of nearby infrastructures such as buildings

The associate editor coordinating the review of this manuscript and approving it for publication was Cheng Chin.

and chimneys, trees, clouds or any foreign materials that act as a barrier between the PV module and irradiance such as leaves, dust, snow, etc., [3]. The occurrence of shading among the PV arrays reduces the performance of the arrays by minimizing the power output equivalent to the power generation of the lowest-performing or shaded modules [4]. The long time existence of partial shading in modules may result in the creation of hotspots formed by the local heat among the cells of the module [5]. This hotspot scenario can physically damage the module by detaching or melting the connectivity wires of cells, breaking the encapsulating glass, burning cells, etc., [6]. The presence of hotspot in the module is mainly detected through various techniques such as infrared thermography [7] whose diagnosis is done by the Naive Bayes classifier [8].

Generally, the modules are integrated with anti-parallel diodes to bypass the current generated by the healthy modules to prevent hotspot formation in shaded cells and enhance the power generation [9]. However, to increase the current generation of the module, turning on the bypass diodes during shading comprises the voltage of the respective modules by forcing them to operate under open-circuit mode [10]. This scenario leads to a voltage imbalance between the modules connected to the array and creates an additional complexity by forming multiple peaks in the characteristics curves of the PV array [11]. The system encounters additional losses caused by the false maximum peak tracking of the maximum power point tracking (MPPT) algorithms. To reduce the losses caused by the false maxima tracking from the P-V or power curves, various hybrid MPPT algorithms have been proposed in a wide range of literature [12]. Some examples of such techniques used for designing hybrid MPPT algorithms include Cuckoo Search [13], Particle Swarm [14], Harris Hawk [15], Grass Hopper [16], Salp Swarm [17], Hybrid Evolutionary [18], Grey Wolf [19], etc. These algorithms use various optimization techniques for searching the actual or global MPP from the non-convex characteristics curves resulting in higher power output and zero losses due to the tracking failure. However, these techniques encounter various limitations in terms of complex algorithms, powerful microcontrollers requirement, need for switches and sensors and reliability of efficient working during all shading patterns.

Arrays are formed by connecting modules in different configurations among which series configuration or long string is highly susceptible to power losses during partial shading and forms a higher number of peaks in the characteristics curves [20]. The partial shading has a puny effect on the performance of parallel-connected modules but, implementation of this configuration is practically avoided due to higher current rating that can result in losses. Hence, the series-parallel (SP) configuration is widely accepted in PV power plants or roof-top systems to effective supply reliable power with desired voltage and current rating to the load. Besides SP, various other configurations such as Bridge-Linked (BL), Honeycomb (HC) and Total Cross Tied (TCT) are formed by connecting wires across the junction of the modules that act as an additional pathway for the higher current to flow without activating the bypass diodes of the shaded modules. The aforementioned configurations are widely tested in simulation and validated experimentally using different shading scenarios for reliability analysis and the study concludes that the TCT configuration has the highest potential of reducing the power losses and enhancing the generation of the array during partial shading [21].

Recently, PV array reconfiguration is gaining wide acceptance in terms of efficient shade mitigation that adopts the concept of distributing the effect of partial shading in the array and hence, reducing the mismatch losses in the system [22]. The PV array reconfiguration is divided into two categories: (a) static reconfiguration, and (b) dynamic reconfiguration. In static reconfiguration, the physical position of the modules is changed to reduce the mismatch among modules whereas, in dynamic reconfiguration, the connections of the modules are changed concerning the shading pattern by using switches [23]. Some of the static reconfiguration strategies include: shade dispersion scheme (SDS) [24], fixed electrical reconfiguration (FER) [25], dominance square (DS) [26], zigzag [27], shade dispersion physical array relocation [28], shade dispersion positioning [29], Sudoku [30], improved Sudoku [31], modified Sudoku [32], competence square [33], magic square [34], etc. These strategies utilize rearrangement concepts or algorithms to change the position of the module to disperse the shading however, changing the module's position requires huge manpower mainly in the case of large power plants that comprise a large number of big size modules. Similarly, various dynamic reconfiguration strategies include: genetic algorithm [33], population-based algorithm [35], two-step GA [36], two-phase array reconfiguration [37], particle swarm optimization [38], modified Harris Hawks optimization [39], swarm reinforcement learning [40], coyote optimization [41], meta-heuristic grasshopper optimization [42], etc. Also, various differential power processing based solutions for reducing the mismatch loss from the partially shaded array have been proposed in a wide range of literature [43]. Some examples include optimized PV-to-bus DPP system [44], power balancing point-based optimization algorithm [45], etc. The afore-mentioned strategies are proved as effective in mitigating the power losses due to partial shading in terms of higher power generation and reduced peak counts as compared to the conventional configurations. However, these techniques encounter a major demerit in terms of implementation as they require a higher number of switches, sensors and powerful microcontrollers that add cost, complexities and additional switching losses to the PV array. Also, these techniques are vulnerable to short-circuit fault that can occur due to the failure of any switches or controllers operating them.

So, in contrast, a reconfiguration technique for the PV arrays has been proposed in this paper that utilizes a one-time electrical connection to reduce the losses that occur due to the presence of partial shading in the system. The superiority of the proposed technique lies in some major aspects such as no sensors, switches, labour or manpower requirements for implementation. The proposed electrical connection can be implemented in PV arrays through an algorithm with the added advantage of being static. The proposed strategy is initially implemented to a 3×3 PV array and compared with the conventional configurations such as series-parallel (SP), bridge-linked (BL), honeycomb (HC), and total cross tied (TCT). Later on, a 9×9 PV array with the conventional configurations, Sudoku repositioning strategy and electrical reconfiguration is considered for comparison. The performance investigation is carried out in MATLAB software and using an experimental prototype under various shading scenarios and the comparison is done using power generation, losses, power curves analysis, efficiencies and performance ratio.
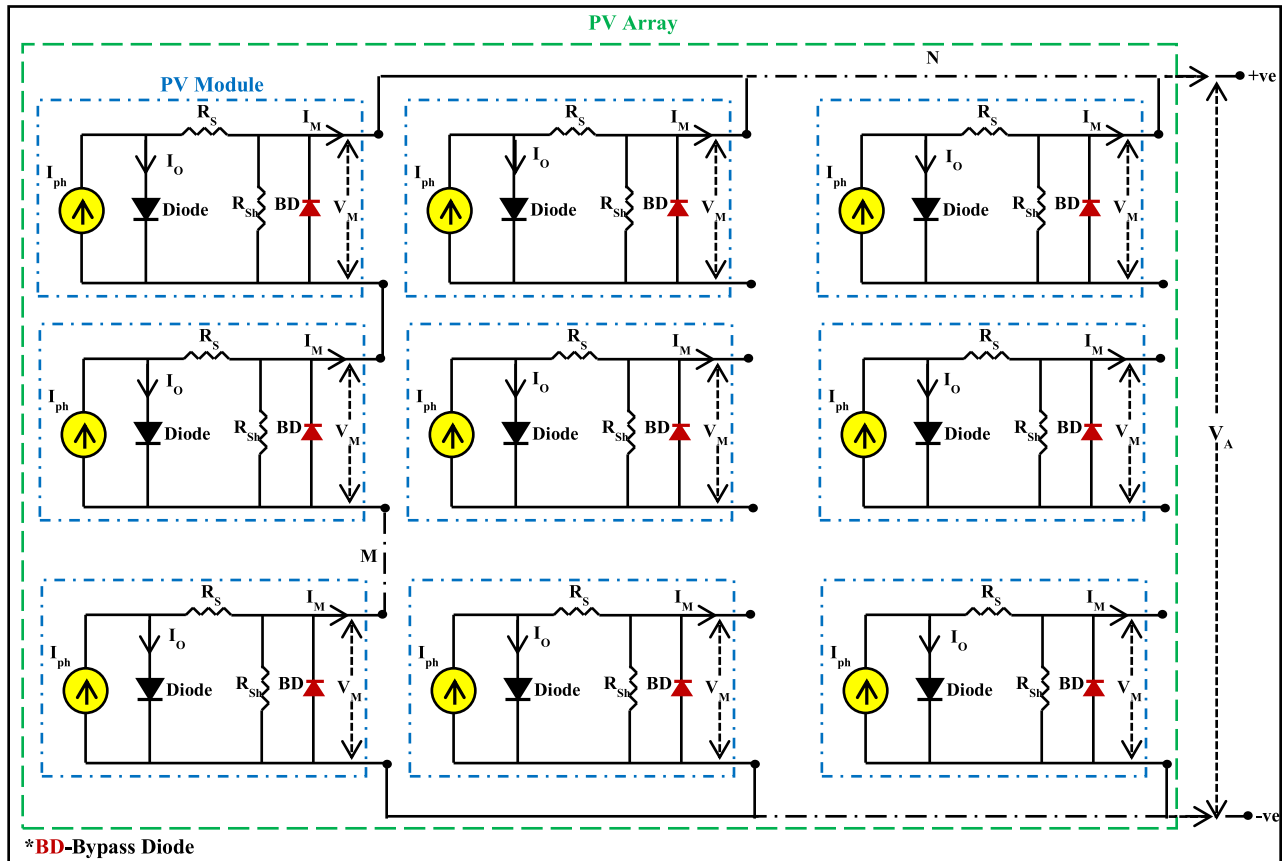
FIGURE 1. Electrical equivalent circuit of PV modules and array.

II. EXISTING SYSTEMS: MODELLING, DESCRIPTION, AND PERFORMANCE PARAMETERS

In this section, the mathematical modelling of the PV array and its configurations and formulations used in the work has been briefly discussed.

A. SIMULATION MODELLING AND EXPERIMENTAL SETUP OF PV ARRAYS

The PV arrays are mainly formed by connecting numerous modules in series and parallel connections to achieve the desired voltage and current rating. The single-diode model is used to mathematically design the modules which are electrically represented by a circuit containing a current source, parallel diode, series resistance (R_S) and shunt resistance (R_{Sh}) in addition to an anti-parallel connected bypass diode. The mathematical equation involved in the modelling of the PV module is represented in equation (1) where I_M, V_M, I_{Ph}, I_O, F and V_T denotes the module's maximum current, maximum voltage, photo-generated current, diode current, ideality factor and thermal voltage respectively.

$$I_M = I_{ph} - I_O \left[\exp\left(\frac{V_M + (R_S \times I_M)}{F \times V_T} \right) - 1 \right] - \frac{V_M + (R_S \times I_M)}{R_{Sh}} \quad (1)$$

The mathematically modelled modules are connected in series and parallel connections to obtain the array whose electrical circuit representation has been depicted in FIGURE 1 where 'M' and 'N' represent the number of rows and columns of the array.

The maximum power of the PV array (P_A) can be determined using the equations (2) where i, j, V_M, I_M, V_A, I_A, M, and N are the rows count, columns count, individual module maximum voltage, individual module maximum current, array maximum voltage, array maximum current, number of rows and number of columns at a given irradiance and operating temperature respectively.

$$P_A = \left[\left\{ \sum_{i=1}^{M} V_M \right\} \times \left\{ \sum_{j=1}^{N} I_M \right\} \right] \quad (2)$$

The specification of the PV module at standard testing condition (STC) i.e. $1000 W/m^2$ receiving irradiance and 25°C operating temperature that used in the work has been given in Table 1. However, to validate the experimental results, the simulation has been conducted based on the real-time environment where the PV module has received the maximum irradiance of $800 W/m^2$ with a module temperature of 45°C during the healthy scenario. The specification of the PV

TABLE 1. Ratings of the PV Module at different conditions, i.e., STC and NOCT.

Parameters	Ratings	
	At STC	*At Field Condition*
Rated Peak Power (PMax)	50W	34.55W
Voltage at Maximum Power (VMP)	17.47V	15.09V
Current at Maximum Power (IMP)	2.866A	2.28A
Open-Circuit Voltage (VOC)	21.566V	19.35V
Shot-Circuit Current (ISC)	3.104A	2.509A
Fill Factor (F.F)	74.69%	71.16%
Efficiency	16.83%	14.54%
Fuse Rating	12A	
Maximum System Voltage	600V	
Dimension	698x666mm	
Power Tolerance	±3%	
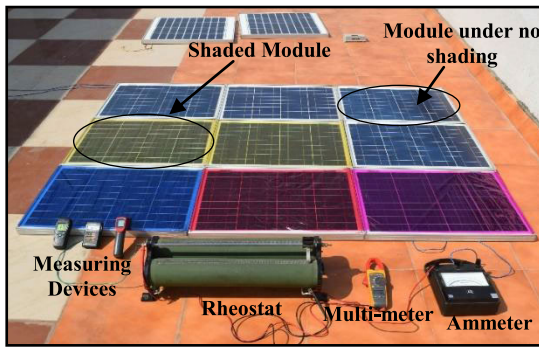
FIGURE 2. Real-time prototype setup for conduction of the experiment.

module based on field condition parameters has been given in Table 1.

The prototype setup for the conduction of experiments in the field scenario has been illustrated in FIGURE 2 where nine modules with the rating given in Table 1 are used to obtain various configurations for the 3 × 3 PV array. The shading scenarios are acquired by applying thin plastic sheets of different colours that act as a barrier between the irradiance and receiving module surface. The PV array has been connected to a variable load (rheostat of 220Ω, and 10A) through an ammeter for current measurement and a multi-meter for voltage measurement. The irradiance received by the modules is measured by two solar power meters whereas an infrared thermometer is used for PV module temperature measurement. The experiment is conducted on the roof of Solar Research Lab, ITER of SOADU from 10:30 AM to 12Noon where the site received an average irradiance of 800-850W/m^2 with an ambient temperature of 34.5°C.

In the simulation, the module has generated power of 35.26W during 800W/m^2 whereas, in the experiment, the power has been recorded as 34.96W with simulation to the experimental error of 0.85%. The simulation and experimental power generation for 600W/m^2 have been recorded as 26.10W and 25.96W respectively with an error of 0.53% whereas, for 450W/m^2, the recorded power values for simulation and experiments are 19.33W and 19.16W respectively with an error of 0.87%. Similarly, during 200W/m^2, the

module has generated 8.12W in simulation and 7.92W in the experiment with an error of 2.42% whereas, for 100W/m^2, the simulation and experimental powers are recorded as 3.83W and 3.75W respectively with an error of 2.08%. The study encountered a minor deviation (<5%) between the power generation data of simulation and experiments due to certain unavoidable factors such as fluctuating irradiance, temperature difference, internal cells mismatch, scratched module glass, and wire losses.

B. PV ARRAY CONFIGURATIONS
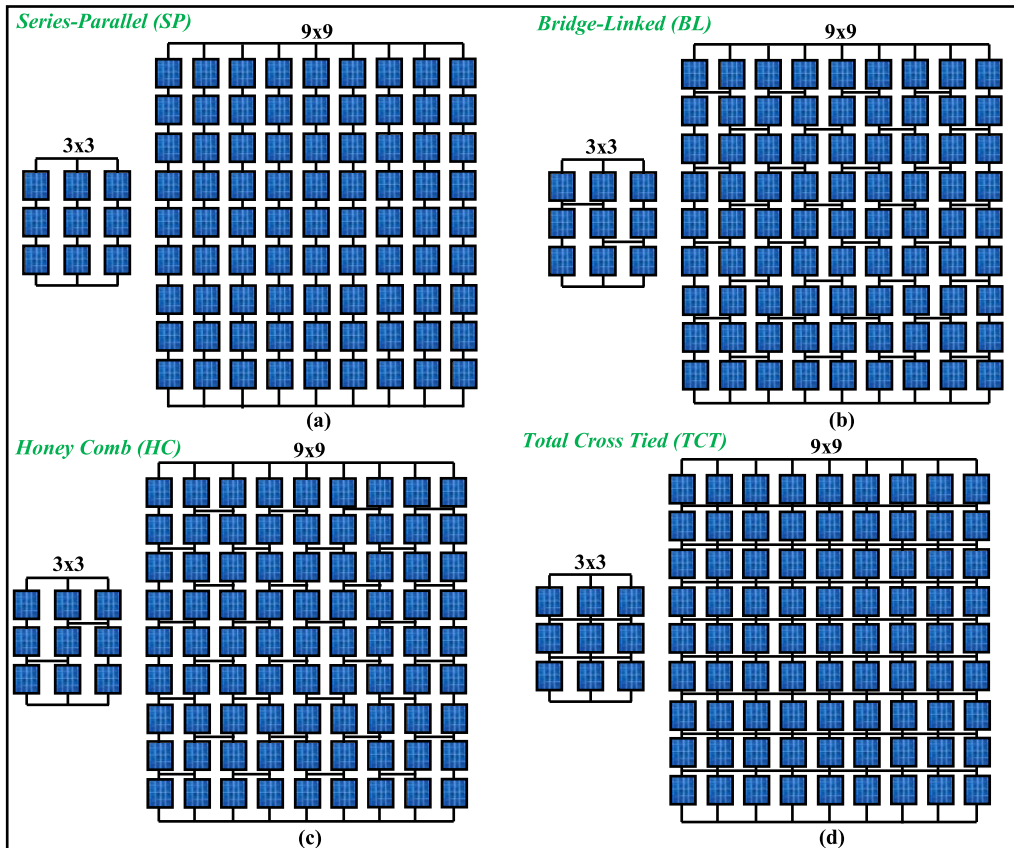#### 1) CONVENTIONAL ARRAY CONFIGURATIONS
The most common and widely used configuration of PV array is series-parallel (SP) where the modules are initially connected in series to increase the voltage forming string and similar strings are connected in parallel to increase the current. However, the series-parallel (SP) configuration encounters the limitation of effective current dispersion during partial shading scenarios that result in severe power losses in the array.

Hence, as a solution to this limitation, the junctions of the SP configured modules are connected with wire ties to provide additional paths for the higher current to flow through preventing bypass diodes activation in the modules under shading. The Bridge-Linked (BL) and Honeycomb (HC) are the configurations with the lowest redundancy where the ties are connected across the module's junction in a bridging manner, however; in the case of total-cross-tied (TCT), the terminals of each module are connected using wire ties. The series-parallel (SP), bridge-linked (BL), honeycomb (HC) and total cross tied (TCT) configurations for 3 × 3 and 9 × 9 PV arrays have been delineated in FIGURE 3 (a), (b), (c) and (d) respectively.

2) SUDOKU RECONFIGURATION TECHNIQUE
The Sudoku reconfiguration [26] is obtained from the logic-based number-placement puzzle where the 9 × 9 array is divided into nine 3 × 3 sub-arrays with the rows and columns containing non-repeating digits from 1 to 9. The initial 9 × 9 array has been given in FIGURE 4 (a) whereas the final renumbered array based on the Sudoku puzzle is depicted in FIGURE 4 (b). In this technique, the physical position of the modules with TCT connection is changed based on the renumbered Sudoku pattern without altering the electrical connection. In the Sudoku technique, the modules located at a single row of TCT configuration are shifted to different rows to minimize the effect of shading occurring at a single row and dispersing it to other rows of the array increases the current entering the node and reduces module bypassing. Taking an example, the position of module 12 (first-row second column) is changed to the seventh-row second column with the module connection remaining in the first row. Similarly, module number 33 (third-row third column) is shifted to the ninth-row third column with an electrical connection remaining at the third row. In this way, the physical position of all the modules

FIGURE 3. Conventional PV array configuration of 3 × 3 and 9 × 9 sizes. (a) Series-parallel (SP), (b) Bridge-linked (BL), (c) Honey comb (HC), and (d) Total cross tied (TCT).

is shifted according to the Sudoku renumbered pattern to disperse the shade throughout the array for power enhancement during shading. As the electrical connection of the array remained unchanged, so, the voltage and current rating remains equal to that of SP, BL, HC and TCT configurations.

C. PERFORMANCE PARAMETERS

The performance of the array configurations is investigated using various measuring parameters to study the efficacy during shading. The array power generation (P_A) is one of the major parameters that can be used for the performance evaluation of the configurations and calculated as

$$P_A = V_A \times I_A \tag{3}$$

The mismatch loss (ML) encountered by the arrays during a particular shading scenario can be calculated from the difference between the power generation of arrays under no shade (P_U) and shaded (P_S) scenarios expressed as

$$ML = P_U - P_S \tag{4}$$

The percentage of power loss (PL) encountered by an array during a particular shading scenario is derived from equation (5) where P_{STC} indicates the array power generation at STC.

$$PL(in\%) = \frac{P_{STC} - P_S}{P_{STC}} \times 100 \tag{5}$$

The efficiency of array configurations (η_{PG}) is calculated using equation (6) in which 'G' and 'A' referred to the irradiance are receiving area of the module respectively.

$$\eta_{PG}(in\%) = \frac{P_S}{G \times A} \times 100 \tag{6}$$

The power conversion efficiency (η_{PC}) is determined by equation (7) where 'P_C' is the calculated power extracted from the sum of power generation of individual PV modules.

$$\eta_{PC}(in\%) = \frac{P_S}{P_C} \times 100 \tag{7}$$

The performance ratio (PR) of the array configurations can be as the percentile ratio of power generation during a shading scenario to an unshaded case and given as

$$PR(in0) = \frac{P_S}{P_U} \times 100 \tag{8}$$

III. ONE-TIME ELECTRICAL RECONFIGURATION: DESCRIPTION, IMPLEMENTATION, AND EVALUATION

The proposed one-time electrical reconfiguration is a permanent solution for partial shading prone arrays which is based on electrical reconnection of the PV modules to disseminate the intensity of partial shading in the array. The main objective of distributing the shading throughout the array is to
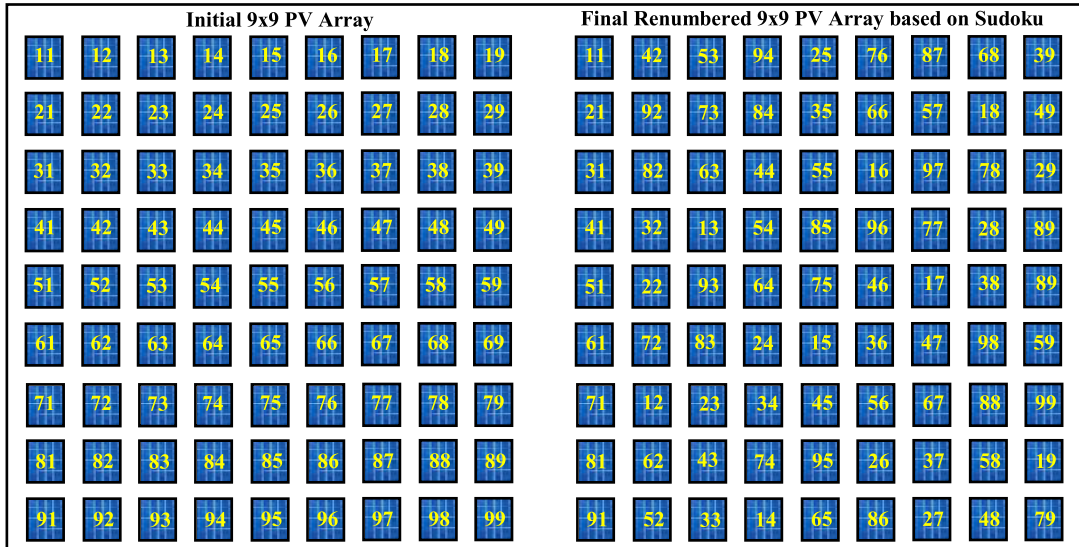
Initial 9x9 PV Array

11	12	13	14	15	16	17	18	19
21	22	23	24	25	26	27	28	29
31	32	33	34	35	36	37	38	39
41	42	43	44	45	46	47	48	49
51	52	53	54	55	56	57	58	59
61	62	63	64	65	66	67	68	69
71	72	73	74	75	76	77	78	79
81	82	83	84	85	86	87	88	89
91	92	93	94	95	96	97	98	99

Final Renumbered 9x9 PV Array based on Sudoku

11	42	53	94	25	76	87	68	39
21	92	73	84	35	66	57	18	49
31	82	63	44	55	16	97	78	29
41	32	13	54	85	96	77	28	89
51	22	93	64	75	46	17	38	89
61	72	83	24	15	36	47	98	59
71	12	23	34	45	56	67	88	99
81	62	43	74	95	26	37	58	19
91	52	33	14	65	86	27	48	79

FIGURE 4. Sudoku technique for 9×9 PV array. (a) Initial array numbering, and (b) Renumbered array based on Sudoku technique.

reduce the possibility of losses caused by the lower current generation in rows of the array.

The reconfiguration initially begins with running the pseudo-code programmed using C++ language as given above that takes the number of rows (M) and columns (N) as input. The program initializes by constructing a matrix Aij of size $M \times N$ with i and j as row and column indices respectively. The output of the program will be a new remembered matrix Bij of the same size $M \times N$ where the numbering of the initially considered matrix is changed by swapping the elements across the rows and columns. After that, a TCT connected array of size $M \times N$ is taken that will act as the guiding reference to carry out the electrical connection of the electrically isolated renumbered array. The detailed steps involved in the implementation of the proposed reconfiguration to a 3×3 array are given in pictorial (FIGURE 5) and explained below.

A. PROGRAM EXECUTION

Step 1: Enter the number of rows and columns of the array as 3 and 3 respectively.

Step 2: The program will initially create a 3×3 PV array (or matrix) with total number of elements equal to 9 that are named according to their row and column indices i.e. 11 (row 1 column 1), 12 (row 1 column 2), 13 (row 1 column 3), 21 (row 2 column 1), 22 (row 2 column 2), 23 (row 2 column 3), 31 (row 3 column 1), 32 (row 3 column 2) and 33 (row 3 column 3) as shown in FIGURE 5 (b).

Step 3: After execution, the program will create a renumbered array (or matrix) based on the shade dispersion logic as shown in FIGURE 5 (c). The modules of the initial 3×3 array are considered to be electrically connected in TCT configuration (FIGURE 5 (d)) whereas the modules of the renumbered PV array are electrically isolated or unconnected with each other.
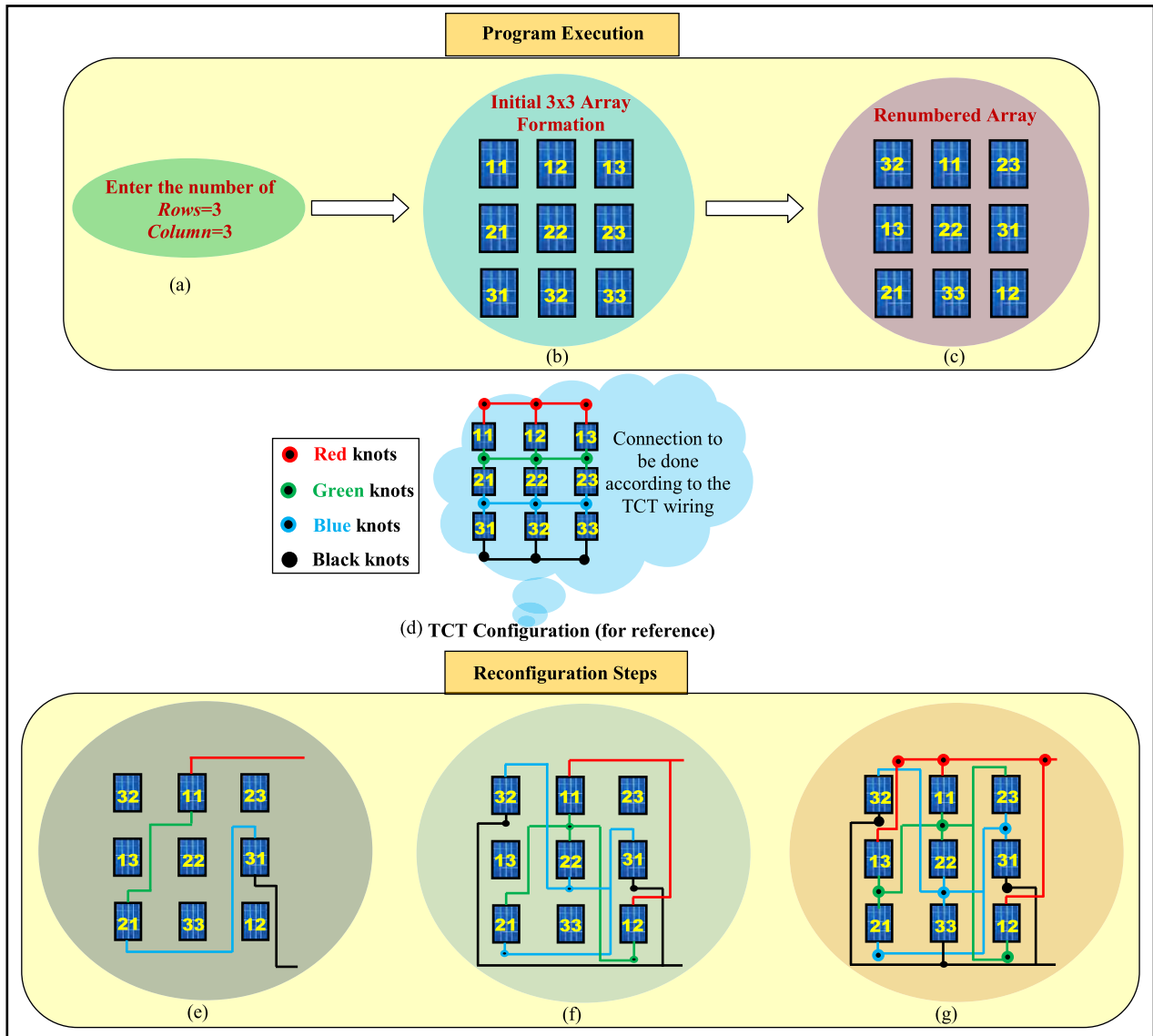
B. ELECTRICAL CONNECTION

Step 4: At first, the modules number 11, 21 and 31 are connected in series [according to the TCT configuration shown in FIGURE 5 (d)] represented by red wires for the positive terminal of module 11, green wires as a connection between module 11 negative and module 21 positive terminals, and blue wires as the connection between module 21 negative and module 31 positive terminals shown in FIGURE 5 (e).

Step 5: Secondly, modules number 12 is connected in parallel with module 11 represented by red (positive) and green (negative) wires and then connected in series with module 22 (green wires as negative of 11 and positive of 22). Similarly, module 22 will be connected in parallel with 21 (green wires) and series with 32 (blue wires) as shown in FIGURE 5 (f).

Step 6: Thirdly, modules number 13 and 12 are connected in parallel (red wires for positive terminals and green wires for negative terminals) and then module 13 is connected in series with 23 (green wires). Similarly, PV module 23 is connected in parallel with module 22 (green wire for positive and blue wire for negative terminals) and series with 33 and then modules 33 and 32 are connected in parallel (blue wire for positive and black wire for negative terminals as shown in FIGURE 5 (g).

For connection simplicity, another approach can be adopted to improve the ease of wiring where the terminals of the PV modules are connected to specific knots of different colours that either connect modules in series or parallel configuration. Considering the connection of the 3×3 renumbered PV array as an example, the positive terminals of modules number 11, 12 and 13 are directly connected to the red knot which is the positive output terminal of the array. The negative terminals of modules 11, 12 and 13, and positive terminals of modules 21, 22 and 12 are connected to the green knot.

FIGURE 5. Detailed steps involved in the implementation of the proposed one-time electrical reconfiguration for a 3 × 3 PV array.

The blue knot has the connections of positive terminals of modules 31, 32, and 33, and negative terminals of modules 21, 22 and 23. The black knot contains the negative terminals of modules 31, 32 and 33 that are connected to the negative output terminal of the PV array. The connection diagram of the renumbered modules for one-time reconfiguration and modules connected to different knots has been shown in FIGURE 6.

Since the wiring of the reconfigured PV array has been done equivalent to the connection of the TCT array, hence, the voltage, current and power ratings of the array with electrical reconfiguration remain the same. In this reconfiguration concept, the modules present in a single row and column of the TCT array are electrically reconnected in such a way that the modules will appear to be at different rows and columns which reduces the chances of shading occurring at a single row and distributes it all over the array. The proposed technique aims to increase the current entering the nodes during shading resulting in an improved power generation of the array.

The proposed reconfiguration strategy has been validated mathematically using a partially shaded 5 × 5 array and compared with the TCT array in terms of theoretical power generation and mismatch losses. The shading scenario applied to the 6 × 6 array with TCT configuration has been depicted in FIGURE.7 (a) where all the modules of the first row received 100W/m^2, and second row received 400W/m^2 and other rows received 1000W/m^2 (unshaded).

The current generated by an individual module at any irradiance level can be mathematically estimated as

$$I_M = \frac{Irradiance}{Irradiance@STC} \times I_{MSTC} = \frac{Irradiance}{1000} \times I_{MSTC}$$
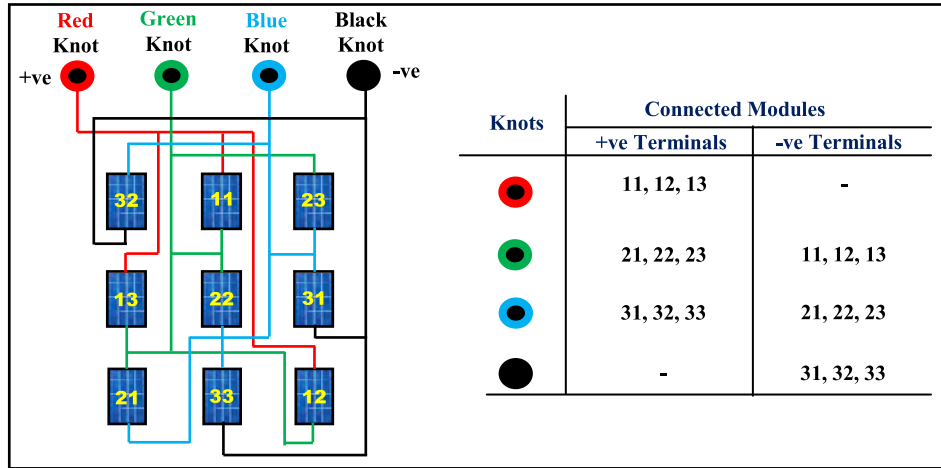
(9)

FIGURE 6. Connection of the terminals of the modules to different knots for ease of implementation of the proposed reconfiguration.
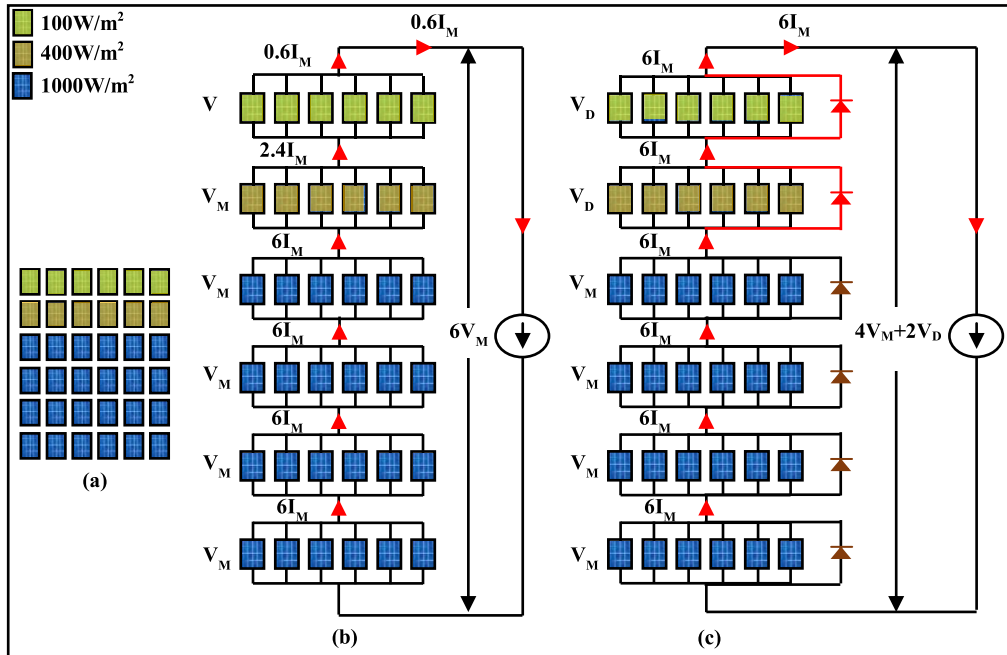

FIGURE 7. Partial shading in a 5 × 5 TCT array. (a) Shading scenario, (b) Current and voltage generation without bypass diodes, and (c) Current and voltage generation with bypass diodes.

In TCT, the modules present in a single row are connected in parallel whereas similar rows are connected in series.

Hence, the current generated by an individual row can be estimated as the sum of individual module current as given in equation (10) whereas the row voltage remains equal to the voltage of a single module.

$$I_R = \sum_{j=0}^{N} I_M = I_M + I_M + I_M + I_M + I_M + I_M = 6I_M \tag{10}$$

Hence, the current generated by the first row (I_{R1}) of the TCT array can be theoretically calculated as

$$I_{R1} = 0.1\, I_M + 0.1\, I_M + 0.1\, I_M + 0.1\, I_M$$

$$|e+ 0.1\, I_M + 0.1\, I_M = 0.6\, I_M \tag{11}$$

Similarly, the current generated by the second row (I_{R2}) of the TCT array can be calculated as

$$I_{R2} = 0.4\, l_M + 0.4\, I_M + 0.4\, I_M + 0.4\, I_M$$
$$+ 0.4\, I_M + 0.4\, I_M = 2.4\, I_M \tag{12}$$

The current generated by the unshaded rows i.e. third (I_{R3}), fourth (I_{R4}), fifth (I_{R5}) and sixth (I_{R6}) of TCT configuration are estimated as

$$I_{R3} = I_{R4} = I_{R5} = I_{R6} = I_M + I_M + I_M$$
$$+ I_M + I_M + I_M = 6I_M \tag{13}$$

C++ Pseudo Code for Renumbering the PV Array

```cpp
#include<iostream>
#include<iomanip>
using namespace std;
void createSquare(int **array, int r, int c) {
    int i, j, count = 1, range;
    for(i = 0; i<r; i++)
        for(j = 0; j<c; j++)
            array[i][j] = 0; //initialize all elements with 0
range = r*c;
i = 0;
j = c/2;
array[i][j] = count;
while(count < range) {
    count++;
    if((i-1) < 0 && (j-1) < 0) //when both row and column
crosses the range
        i++;
    else if((i-1) <0) {//when only row crosses range, set i to
last row, and decrease j
        i = r-1;
        j--;
    }else if((j-1) < 0) {//when only col crosses range, set j to
last column, and decrease i
        j = c-1;
        i--;
    }else if(array[i-1][j-1] != 0) //when diagonal element is
not empty, go to next row
        i++;
    else{
        i--;
        j--;
    }
    array[i][j] = count;
}
// Printing the array
for(i = 0; i<r; i++) {
    for(j = 0; j<c; j++)
        cout <<setw(3) << array[i][j];
    cout << endl;
} }
main() {
    int** matrix;
    int row, col;
    cout << "Enter the size of PV array:";
    cin >> row;
    col = row;
    matrix = new int*[row];
    for(int i = 0; i<row; i++) {
        matrix[i] = new int[col];
    }
    createSquare(matrix, row, col);
}
```

Considering the TCT PV array with modules having no bypass diodes (as shown in FIGURE 7 (b)), the maximum

current output (I_{ATCT}) of the array will be the current output of the lowest-performing modules (series current limitation) i.e. $0.6I_M$ whereas the maximum voltage output (V_{ATCT}) will be equal to $6V_M$. Hence, the maximum power output of the TCT without bypass diodes can be theoretically calculated as

$$P_{ATCT} = V_{ATCT} \times I_{ATCT} = 6V_M \times 0.6 I_M = 3.6 V_M I_M \quad (14)$$

In a TCT array with bypass diodes (as shown in FIGURE 7 (c)), the maximum current output (I_{ATCT}) of the array will be $6I_M$ as the current generated by the unshaded modules flows through the bypass diodes without flowing through the shaded modules. However, turning on bypass diodes result in voltage reduction of the respective module's row (open-circuit of modules) equivalent to the forward-biased voltage of the bypass diode, i.e., V_D. Hence, two rows of the TCT array are forwarded generating a voltage of V_D by each row resulting in a total array voltage equal to $4V_M+2V_D$. Hence, the total power output of the TCT array with bypassing the shaded rows considering $V_D \lll V_M$ and can be theoretically calculated as

$$P_{ATCT} = V_{ATCT} \times I_{ATCT} = 4V_M \times 6 I_M = 24V_M l_M \quad (15)$$

The shade dispersion in the case of the proposed electrical reconfiguration has been shown in FIGURE 8 (a) where the shading present over the first two rows of the TCT is distributed throughout the PV array. The maximum current generation of the rows can be mathematically calculated as

$$I_{R1} = I_{R3} = I_{R5} = 0.1 I_M + I_M + I_M + 0.1 I_M$$
$$+ I_M + I_M = 4.2 I_M \quad (16)$$
$$I_{R2} = I_{R4} = I_{R6} = I_M + 0.4 I_M + I_M + 0.4 I_M$$
$$+ I_M + I_M = 4.8 I_M \quad (17)$$

Hence, the maximum power output of the PV array with the proposed one-time electrical reconfiguration (P_{AE}) and no bypass diodes [FIGURE 8 (b)] can be calculated as

$$P_{AE} = V_{AE} \times I_{AE} = 6V_M \times 4.2 I_M = 25.2 V_M I_M \quad (18)$$

Similarly, the power output of one-time reconfiguration array with bypass diodes has been calculated as

$$P_{AE} = V_{AE} \times I_{AE} = 3V_M \times 4.8 I_M = 14.4 V_M I_M \quad (19)$$

But, practically turning on the bypass diodes scenario is limited as shaded modules bypassing mainly occurs when the power generated by the modules under no shade is higher than the net power generation of the array. Hence, for reduced complexity, the power generation of the PV arrays without bypassing the shaded modules is considered for comparison.

The maximum power generation of the 6×6 PV array during no shading/ healthy scenario can be calculated as

$$P_A = V_A \times I_A = 6V_M \times 6I_M = 36V_M I_M \quad (20)$$
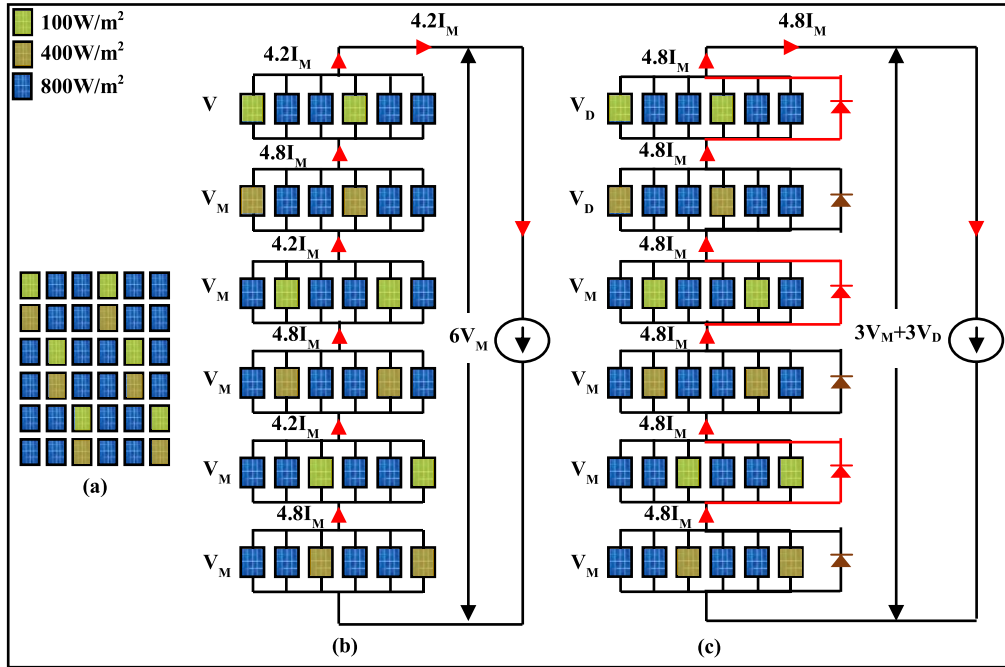
FIGURE 8. Partial shading in a 5 × 5 array with proposed reconfiguration. (a) Shading scenario, (b) Current and voltage generation without bypass diodes, and (c) Current and voltage generation with bypass diodes.

The total power losses encountered by the PV array with TCT configuration (P_{LossT})) can be calculated as

$$P_{LossT} = P_A - P_{ATCT} = 36 V_M I_M - 3.6\ V_M I_M$$
$$= 32.4\ V_M I_M \quad (21)$$

Similarly, the power losses encountered by the array with proposed one-time electrical reconfiguration (P_{LossE}) can be calculated as

$$P_{LossE} = P_A - P_{AE} = 36 V_M I_M - 25.2\ V_M I_M$$
$$= 10.8\ V_M I_M \quad (22)$$

Hence, from equations (21) and (22), it can be observed that the PV array with the proposed one-time electrical reconfiguration has reduced the power losses up to $21.6 V_M I_M$ as compared to the TCT array. Also, it can be stated that the proposed one-time electrical reconfiguration has generated 85.71% higher power as compared to the TCT configuration during this particular shading scenario which reflects the efficacy of the proposed strategy in terms of higher power generation.

IV. SIMULATION AND EXPERIMENTAL RESULTS: ANALYSIS AND DISCUSSIONS

The proposed one-time electrical reconfiguration has been tested using two different array sizes i.e. 3 × 3 and 9 × 9 and compared with various configurations such as series-parallel (SP), bridge-linked (BL), honeycomb (HC), total cross tied (TCT) and Sudoku reconfiguration (for 9 × 9 PV array). The entire investigation is conducted in the MATLAB software and prototype field experimental setup (for 3 × 3 PV array).

The rating of the PV module considered for the simulation and experimental analysis of the 3 × 3 array has been tabulated in Table 1. However, the 9 × 9 PV array has been studied only in the simulation environment using large size PV modules generating a maximum power output of 325W, maximum voltage: 37.8V, maximum current: 8.60A, open-circuit voltage:46.60V and short-circuit current: 9.20A at STC.

The comparison of the configurations has been done using various parameters given in equations (4)-(9) such as power generation, mismatch loss, power loss, power generation efficiency, power conversion efficiency and performance ratio. The analysis has been carried out using different shading scenarios that differ in terms of size, strength and pattern where the modules under no shading condition are operated at 800W/m^2 irradiance and 50°C module temperature (based on real-time environment data) and the shaded modules received different levels of irradiances i.e. 100W/m^2, 200W/m^2, 400W/m^2 and 600W/m^2. The maximum power generated by the unshaded 3 × 3 and 9 × 9 arrays in the simulation at 800W/m^2 and 50°C has been found as 317.61W and 22894.55W respectively.

A. SCENARIO A

The shading for the PV arrays with SP, BL, HC, TCT and proposed one-time reconfiguration has been depicted in FIGURE 9 (a). During this particular shading, the modules present in the first-row first-column, first-row second-column, second-row first-column and second-row second column are subjected to receive lower irradiance levels of 100W/m^2, 100W/m^2, 200W/m^2 and 200W/m^2 respectively.
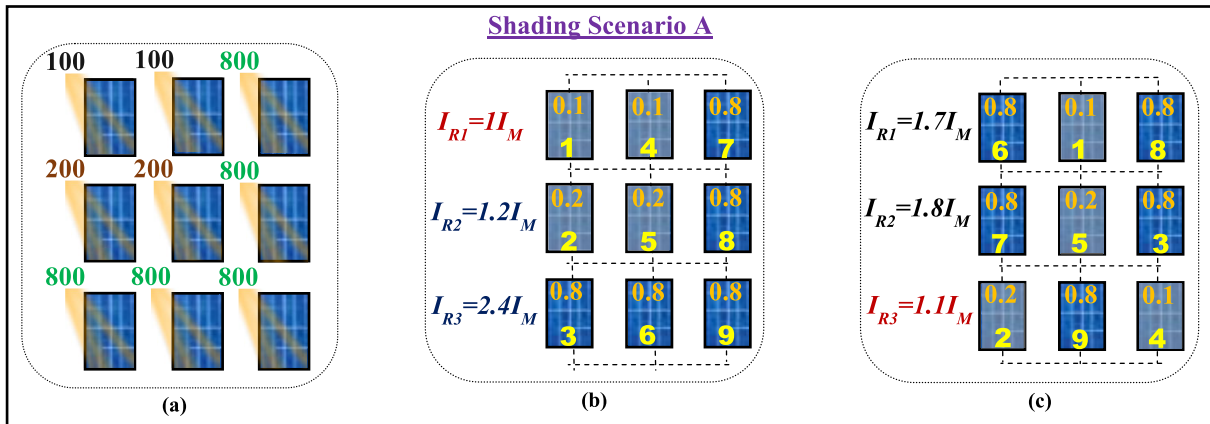
FIGURE 9. Partial shading in 3 × 3 PV Array. (a) Partial shading scenario A, (b) Shading and row current estimation in TCT configuration and, (c) Shade dispersion and row current estimation by one-time electrical reconfiguration (proposed).

TABLE 2. Mathematical evaluation of current, voltage, power and location of GMPP during shading scenario a for TCT and proposed one-time reconfiguration.

TCT Configuration			Proposed One-time Electrical Reconfiguration		
Row Currents	*Voltage*	*Power*	*Row Currents*	*Voltage*	*Power*
I_{R1} $1I_M$	$3V_M$	**$3V_MI_M$**	I_{R1} $1.7I_M$	$3V_M$	**$5.1V_MI_M$**
I_{R2} $1.2I_M$	$2V_M$	$2.4V_MI_M$	I_{R2} $1.8I_M$	$2V_M$	$3.6V_MI_M$
I_{R3} $2.4I_M$	V_M	$2.4V_MI_M$	I_{R3} $1.1I_M$	V_M	$1.1V_MI_M$

The total available power from the array during this shading scenario has been calculated as 200.2W (simulation) and 198.14W (experiment). The rows currents estimation for the TCT configuration has been shown in FIGURE 9 (b) in which the theoretical currents generation of the array has been estimated as $1I_M$ (first row), $1.2I_M$ (second row) and $2.4I_M$ (third row) respectively. Similarly, the theoretical rows current generated by the array with proposed one-time reconfiguration (FIGURE 9 (c)) has been calculated as $1.7I_M$ for the first row, $1.8I_M$ for the second row and $1.1I_M$ for the third row.

The theoretical estimation of the array current, voltage and power based on the bypassing of shaded rows in case of TCT and proposed one-time electrical reconfiguration have been tabulated in Table 2. From the table, it can be seen that the location of the global maximum power point (GMPP) of TCT is at $3V_MI_M$.

In the case of one-time reconfiguration, the GMPP lies at a higher position i.e. $5.1V_MI_M$ which reflects the higher power generation of the array with the proposed strategy.

The power curves of the arrays with SP (blue curve), BL (green curve), HC (red curve), TCT (pink curve), and proposed one-time electrical reconfiguration (black curve) obtained from the simulation analysis have been shown in FIGURE 10. The power generation of the array with SP, BL, HC and TCT configuration during shading scenario A have been found as 134.55W, 141.32W, 140.15W, and 144.71W respectively. The array with the proposed reconfiguration strategy has a higher power generation of 160.61W as the intensity of the shading in a particular row gets

dispersed all over the array resulting in higher power generation. The mismatch losses (ML) encountered by the SP, BL, HC and TCT configurations have been calculated as 183.06W, 176.29W, 177.46W and 167.9W, with power losses of 70.1%, 68.59%, 68.85% and 67.84% respectively. The power generation efficiencies (η_{PG}) of the configurations have been calculated as 6.31% (SP), 6.63% (BL), 6.57% (HC), and 6.79% (TCT) whereas the power conversion efficiencies (η_{PC}) are calculated as 67.20% (SP), 70.58% (BL), 70% (HC) and 72.29% (TCT). However, the array with the proposed one-time electrical reconfiguration encountered the lowest losses of 157W (mismatch) and 64.30% (power) with 7.53% (power generation efficiency) and 80.22% (power conversion efficiency) than the SP, BL, HC and TCT configurations. The proposed strategy has shown a superior performance (50.56%) by generating notably higher power than the SP (42.36%), BL (44.49%), HC (44.12%) and TCT (45.57%) configurations. An experiment has been carried out with the shading scenario A for the 3 × 3 array configurations and the power curves obtained (data from experiments and plotted in MATLAB) are depicted in FIGURE 11. The maximum power of SP, BL, HC, TCT and one-time electrical reconfiguration obtained from the experiments has been measured as 132.86W, 139.7 2W, 138.27W, 142.71W and 158.76W respectively. Hence, from the above simulation and experimental analysis, it has been observed that the proposed one-time reconfiguration improved the array performance with a higher power output of 19.36%, 13.64%, 14.59% and 10.96% higher power than SP, BL, HC and TCT respectively.
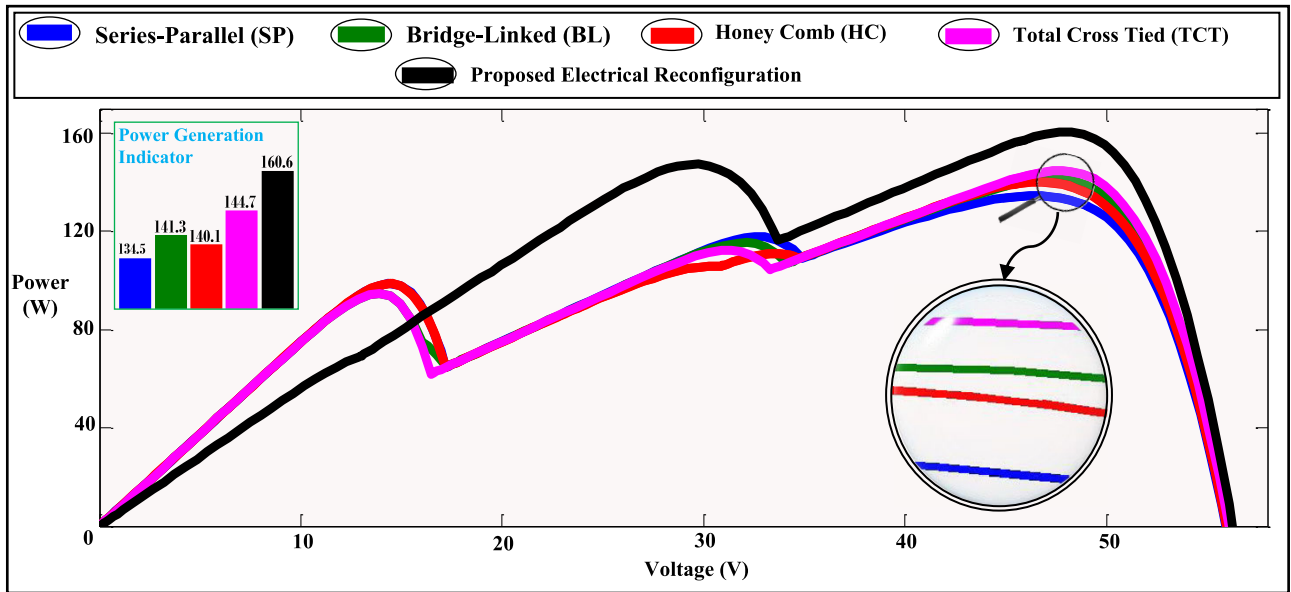
FIGURE 10. Power curves of the PV arrays (SP, BL, HC, TCT configurations) and One-time electrical reconfiguration) during partial shading scenario A (simulation analysis).
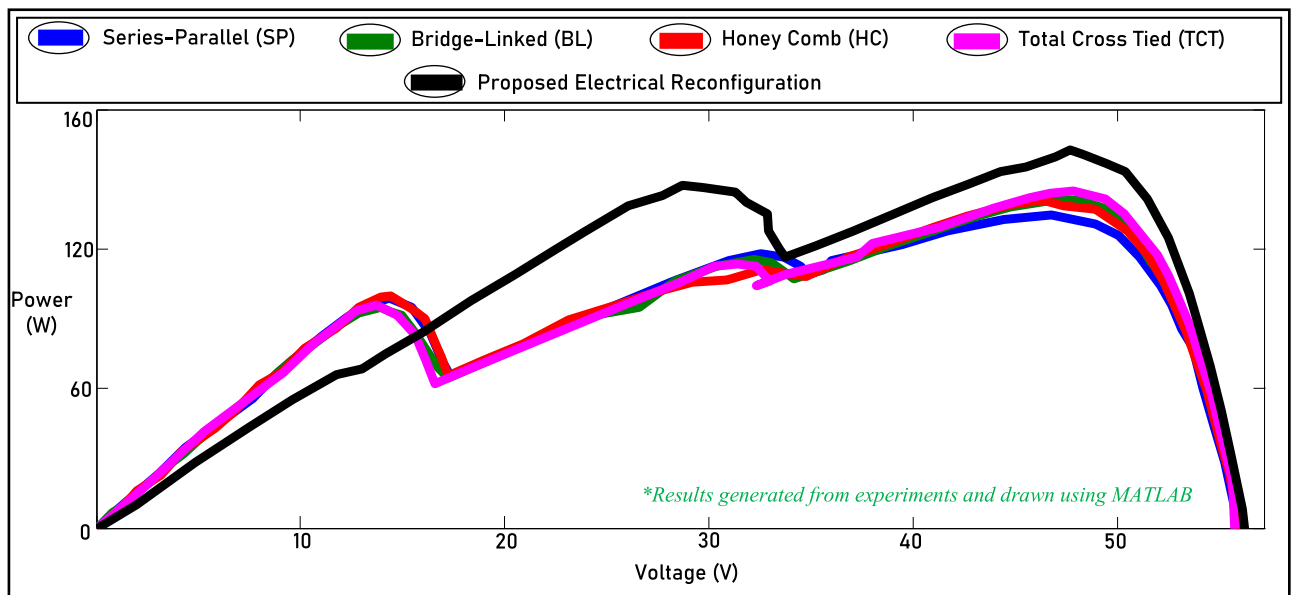

FIGURE 11. Power curves of the PV arrays (SP, BL, HC, TCT configurations) and One-time electrical reconfiguration) during partial shading scenario A (experimental analysis).

B. SCENARIO B

The shading scenario B has been shown in FIGURE 12 (a) where all the three rows of the arrays are subjected to partial shading with the first two modules of the first-row, second-row and third-row (from the left side view) receiving lower irradiances ($400W/m^2$, $600W/m^2$ and $200W/m^2$ respectively) whereas the unshaded modules (last modules of each row) received $800W/m^2$. The shading structure in the case of the TCT array has been shown in FIGURE 12 (b) and the shade dispersion by the one-time electrical reconfiguration has been

displayed in FIGURE 12 (c) along with the rows' current estimation. The theoretical currents of row 1, row 2 and row 3 in the TCT array have been estimated as $1.6I_M$, $2I_M$ and $1.2I_M$ respectively whereas the reconfigured array has rows current estimated as $1.4I_M$ (row 1), $1.6I_M$ (row 2) and $1.8I_M$ (row 3).

The theoretical current, voltage and power estimations of the array with TCT configuration and one-time electrical reconfiguration during scenario B have been calculated and given in Table 3. It can be observed from the table that the GMPP in the case of TCT i.e. $3.2V_MI_M$ can be achieved only
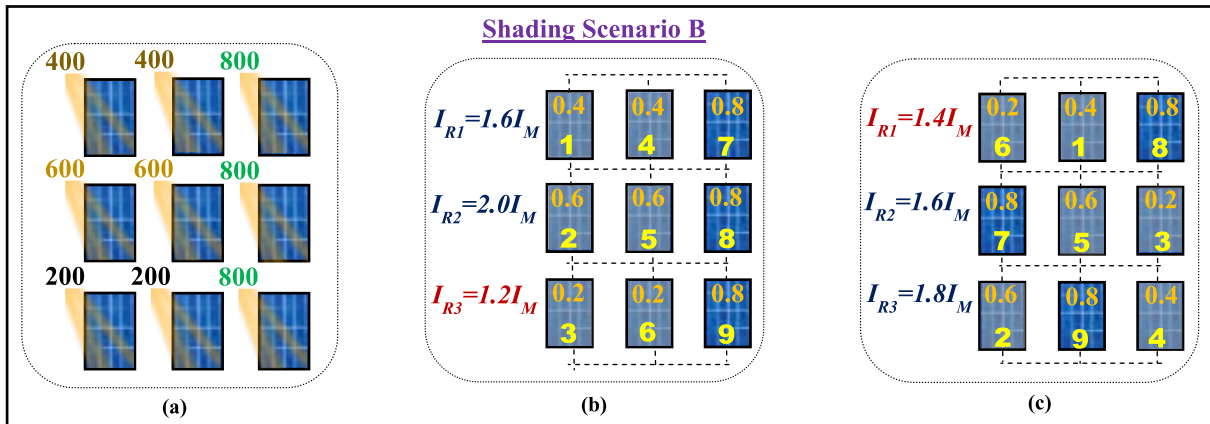
FIGURE 12. Partial shading in 3 × 3 PV array. (a) Partial shading scenario B, (b) Shading and row current estimation in TCT configuration and, (c) Shade dispersion and row current estimation by one-time electrical reconfiguration (proposed).

TABLE 3. Mathematical evaluation of current, voltage, power and location of GMPP during shading scenario b for TCT and proposed one-time reconfiguration.

TCT Configuration				Proposed One-time Electrical Reconfiguration		
Row Currents		*Voltage*	*Power*	*Row Currents*		*Voltage*	*Power*
I_{R3}	$1.2I_M$	$3V_M$	$2.4V_MI_M$	I_{R3}	$1.8I_M$	$3V_M$	$5.4V_MI_M$
I_{R1}	$1.6I_M$	$2V_M$	$3.2V_MI_M$	I_{R1}	$1.4I_M$	$2V_M$	$2.8V_MI_M$
I_{R2}	$2.0I_M$	V_M	$2.0V_MI_M$	I_{R2}	$1.4I_M$	V_M	$1.4V_MI_M$

after bypassing one complete row of the array however, the GMPP of the array with reconfiguration has been extracted without bypassing any row of the array at $5.4V_MI_M$. The power curves (simulation) of the PV array configurations including SP, BL, HC, TCT and proposed reconfiguration have been shown in FIGURE 13 where it can be visualized that the curve of the proposed reconfiguration (black curve) lies at the higher position indicating higher power generation than others.

The total available power from the PV array has been calculated as the sum of individual module power generation and found as 212.22W. The PV array with the electrical reconfiguration has generated a notable higher power output (196.66W) followed by the TCT (174.37W), BL (173.59W), HC (167.53W) and SP (163.89W). The SP experienced the highest losses of 153.72W (mismatch) and 63.58% (power) followed by HC (50.08W, 62.77%), BL (144.02W, 61.42%) and TCT (143.24W, 61.25%) whereas the electrical reconfiguration array encountered a minimal mismatch and power losses of 120.95W and 56.2% respectively. Taking the power generation and conversion efficiencies into account, the proposed electrical reconfiguration has the higher efficiencies (9.22% generation and 92.66% conversion) as compared to TCT (8.18% generation and 82.16% conversion), BL (8.14% generation and 81.79% conversion), HC (7.86% generation and 78.94% conversion) and SP (7.69% generation and 77.22% conversion) configurations. Hence, it can be concluded that the proposed strategy has better performance (61.91) during shading scenario B as compared to the TCT (54.90%), BL (54.65%), HC (52.74%) and SP

(51.60%) configurations. Also, there is a power enhancement in the PV array with proposed reconfiguration concerning SP (19.99%), BL (13.28%), HC (17.38%) and TCT (12.18%) configurations.

C. SCENARIO C
During this shading scenario (FIGURE 14 (a)), the modules present in the first row of the array are operated under no shading scenario receiving $800W/m^2$ whereas the first two modules of the second row (from the left side view) received $400W/m^2$, first two modules of third-row received $200W/m^2$ and the third modules of second and third rows received $600W/m^2$.

The shading scenario C occurrence in the case of the TCT array has been delineated in FIGURE 14 (b) whereas the shade dispersion by the one-time electrical reconfiguration strategy has been shown in FIGURE 14 (c).

The row's current estimation of the TCT array has been mathematically calculated as $2.4I_M$ for the first row, $1.4I_M$ for the second row and $1I_M$ for the third row. Similarly, the row current estimation of the array with proposed reconfiguration for shading scenario C has been mathematically calculated as $1.6I_M$, $1.4I_M$, and $1.8I_M$ for the first, second and third rows respectively. The theoretical current, voltage and power calculation of the array with TCT configuration and proposed reconfiguration has been tabulated in Table 4. From the table, it can be observed that the PV array with TCT configuration has the theoretical GMPP at $3V_MI_M$ whereas the proposed reconfiguration has a notable higher GMPP lying at $5.4V_MI_M$.

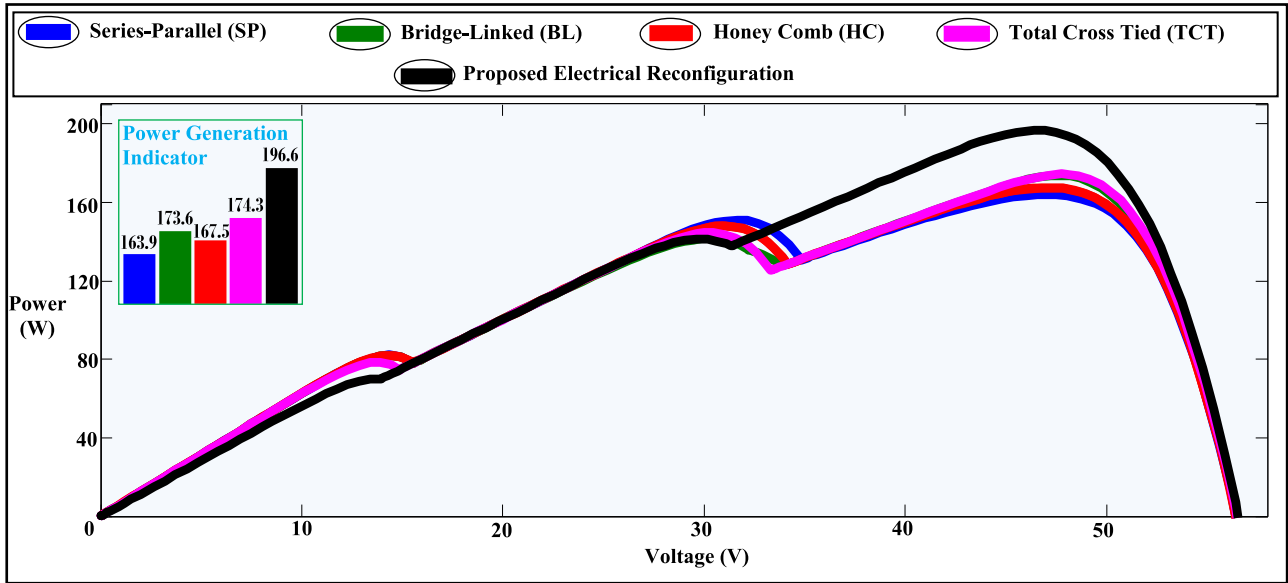**FIGURE 13.** Power curves of PV arrays (SP, BL, HC, TCT configurations) and One-time electrical reconfiguration) during partial shading scenario B (simulation analysis).
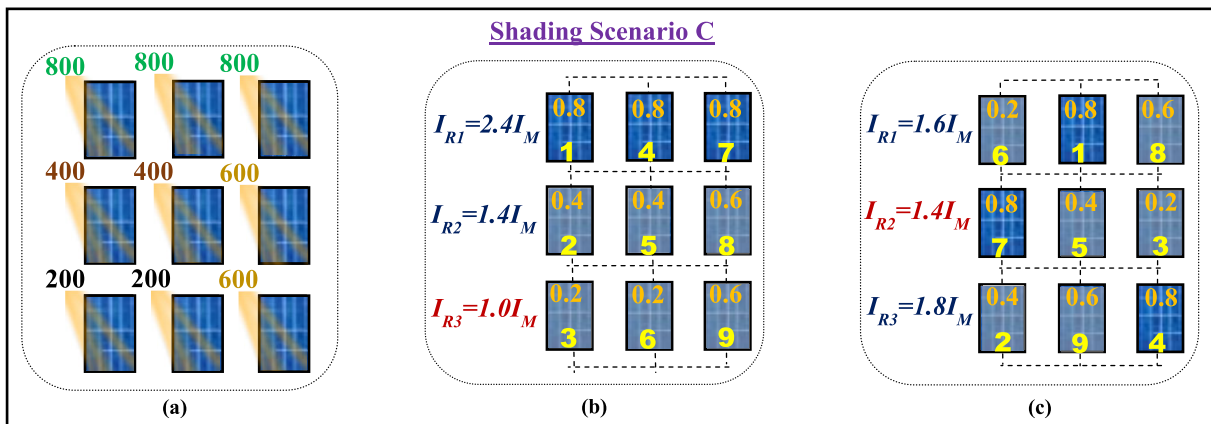

FIGURE 14. Partial shading in 3 × 3 PV Array. (a) Partial shading scenario C, (b) Shading and row current estimation in TCT configuration and, (c) Shade dispersion and row current estimation by one-time electrical reconfiguration (proposed).

TABLE 4. Mathematical evaluation of current, voltage, power and location of GMPP during shading scenario C for TCT and proposed one-time reconfiguration.

TCT Configuration			Proposed One-time Electrical Reconfiguration		
Row Currents	*Voltage*	*Power*	*Row Currents*	*Voltage*	*Power*
I_{R3} $1I_M$	$3V_M$	**$3V_MI_M$**	I_{R3} $1.8I_M$	$3V_M$	**$5.4V_MI_M$**
I_{R2} $1.4I_M$	$2V_M$	$2.8V_MI_M$	I_{R3} $1.4I_M$	$2V_M$	$2.8V_MI_M$
I_{R1} $2.4I_M$	V_M	$2.4V_MI_M$	I_{R1} $1.6I_M$	V_M	$1.6V_MI_M$

The power curves of the PV array are represented in FIGURE 15 (simulation generated) in which the proposed reconfiguration has generated a notably higher power of 196.65W (curve located at a higher position) as compared to the TCT (147.40W), BL (146.42W), HC (143.35W) and SP (141.20W) configurations. The mismatch losses are calculated as 1178.26W (SP), 173.11W (BL), 177.12W (HC) and 172.31W (TCT) and the power losses are calculated

as 69.03% (SP), 67.88% (BL), 68.78% (HC) and 67.71% (TCT). Also, power generation and conversion of efficiencies of the TCT (6.81% and 68.46%) are higher as compared to SP (6.53% and 65.66%), BL (6.78% and 68.08%) and HC (6.59% and 66.20%). However, the proposed reconfiguration strategy encountered the lowest mismatch (122.95W) and power (56.74%) losses with higher power generation (9.13%) and conversion (91.72%) efficiencies. Hence, it can
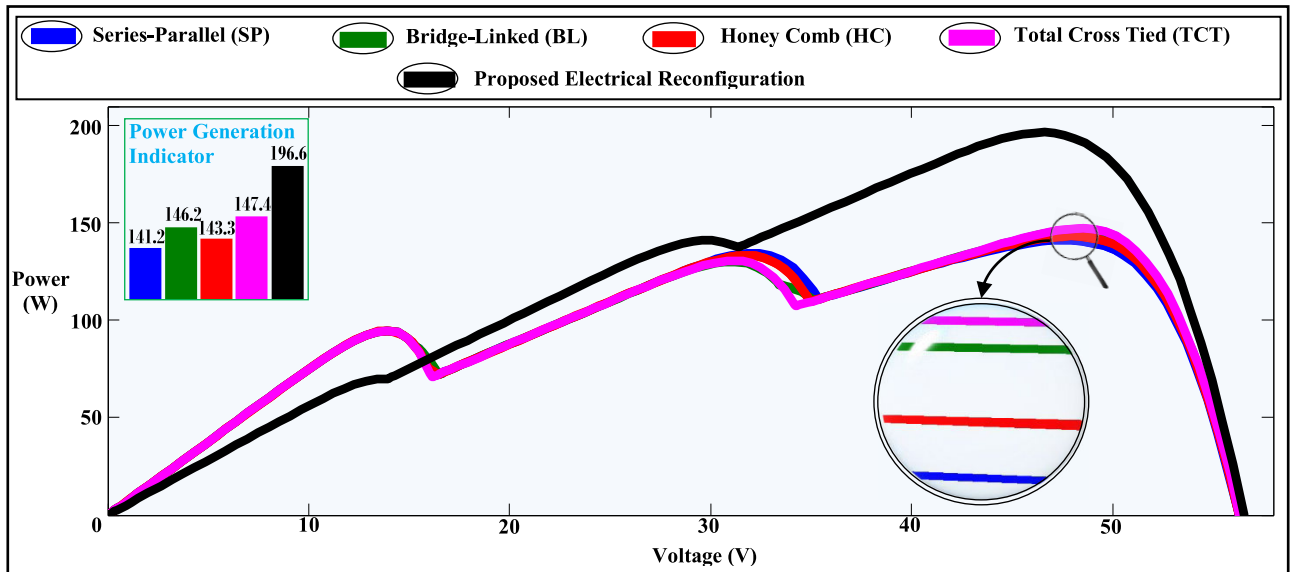
FIGURE 15. Power curves of PV arrays (SP, BL, HC, TCT configurations) and One-time electrical reconfiguration) during partial shading scenario C (simulation analysis).
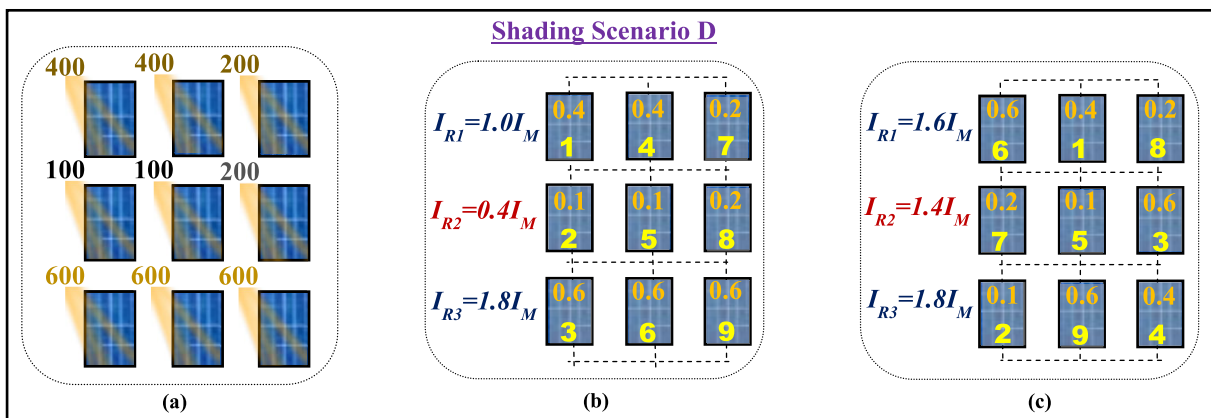

FIGURE 16. Partial shading in 3 × 3 PV Array. (a) Partial shading scenario D, (b) Shading and row current estimation in TCT configuration and, (c) Shade dispersion and row current estimation by one-time electrical reconfiguration (proposed).

be stated that the proposed strategy has higher performance (61.28%) as compared to the TCT (45.74%), BL (45.49%), HC (44.23%) and SP (43.87%) configurations. The proposed strategy has significantly generated 39.69% higher power than SP, 34.71% than BL, 35.50% than HC and 32.06% than TCT during this particular shading scenario.
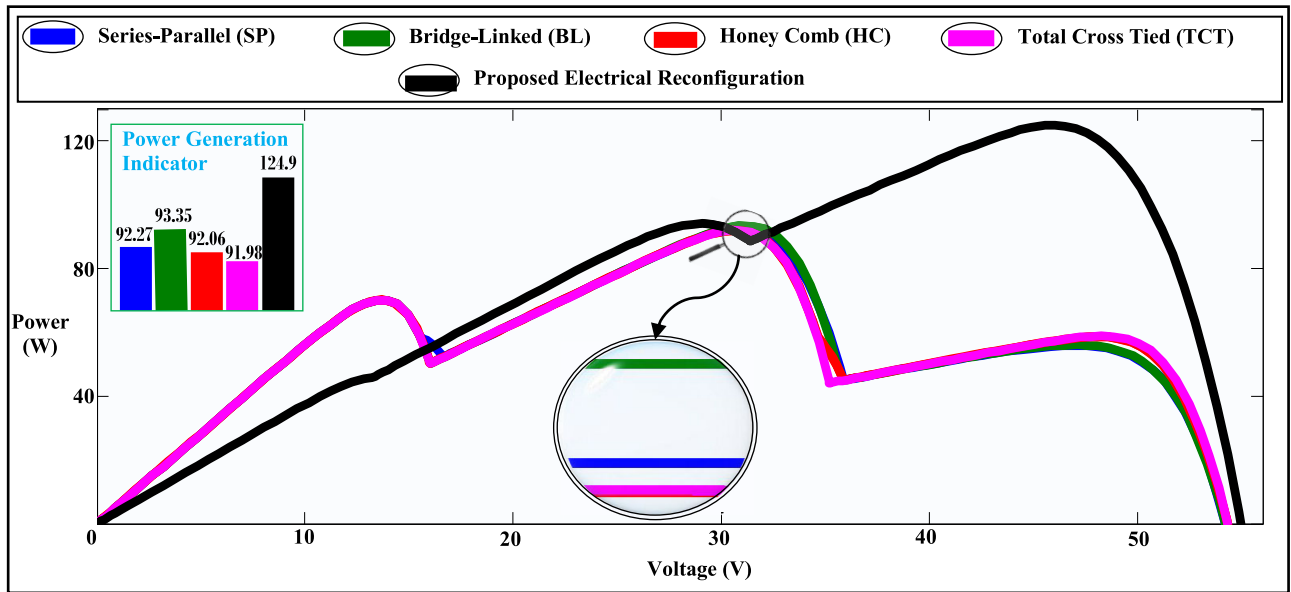
D. SCENARIO D

The shading scenario D is shown in FIGURE 16 (a) in which the whole array is under shading receiving lower irradiances of $100W/m^2$, $200W/m^2$, $400W/m^2$ and $600W/m^2$. This scenario is considered to be one of the complex scenarios as besides the available irradiance of $800W/m^2$, the PV array operates under more than three irradiance levels. The rows currents in the TCT configuration have been theoretically calculated as $1I_M$ (Row 1), $0.4I_M$ (Row 2) and $1.8I_M$ (Row 3) as shown in FIGURE 16 (b). Similarly, theoretical currents

generated by the array after shade dispersion by the proposed strategy for row1, row 2 and row 3 have been calculated as $1.6I_M$, $1.4I_M$ and $1.8I_M$. The theoretical estimation of row currents, voltage and power of the PV arrays with TCT configuration and proposed reconfiguration are calculated and tabulated in Table 5. It can be observed that the GMPP ($2V_MI_M$) of TCT can be acquired after bypassing one row of the array whereas the GMPP of the array with the proposed strategy occurred without bypassing any row i.e. $4.2V_MI_M$.

The power graphs of the configurations and proposed electrical reconfiguration are depicted in FIGURE 17 and the calculated power has been calculated as 140.2W. The electrical reconfiguration has significantly increased the power generation of the PV array by generating maximum power of 124.99W as compared to the SP (92.27W), BL (93.35W), HC (92.06W) and TCT (91.98W) configurations. The reconfigured array experienced the lowest losses of 192.62W

TABLE 5. Mathematical evaluation of current, voltage, power and location of GMPP during shading scenario D for TCT and proposed one-time reconfiguration.

TCT Configuration			Proposed One-time Electrical Reconfiguration		
Row Currents	*Voltage*	*Power*	*Row Currents*	*Voltage*	*Power*
I_{R2} $\quad$ $0.4I_M$	$3V_M$	$1.2V_MI_M$	I_{R3} $\quad$ $1.4I_M$	$3V_M$	**4.2V_MI_M**
I_{R1} $\quad$ $1.0I_M$	$2V_M$	**2.0V_MI_M**	I_{R3} $\quad$ $1.6I_M$	$2V_M$	$2.8V_MI_M$
I_{R3} $\quad$ $1.8I_M$	V_M	$1.8V_MI_M$	I_{R1} $\quad$ $1.8I_M$	V_M	$1.6V_MI_M$

FIGURE 17. Power curves of PV arrays (SP, BL, HC, TCT configurations) and One-time electrical reconfiguration) during partial shading scenario D (simulation analysis).

(mismatch) and 72.22% (power) with notably higher power generation and conversion efficiencies of 5.84% and 89.15% respectively. The SP configuration has experienced losses of 225.34W (mismatch) and 79.49% (power) as compared to the BL (224.26W and 79.25%), HC (225.55W and 79.54%) and TCT (225.63W and 79.56%) configurations. Also, the power generation and conversion efficiencies of SP, BL, HC and TCT are calculated as 4.32% and 65.81%, 4.38% and 66.58%, 4.31% and 65.66%, and 4.31% and 65.58% respectively. The performance ratios of the SP, BL, HC, TCT and proposed reconfiguration have been calculated as 29.05%, 29.39%, 28.98%, 28.96% and 39.35% respectively. From the results, it has been found that there is a power enhancement of 35.46%, 33.89%, 35.77% and 35.88% in the reconfigured array than SP, BL, HC and TCT respectively.
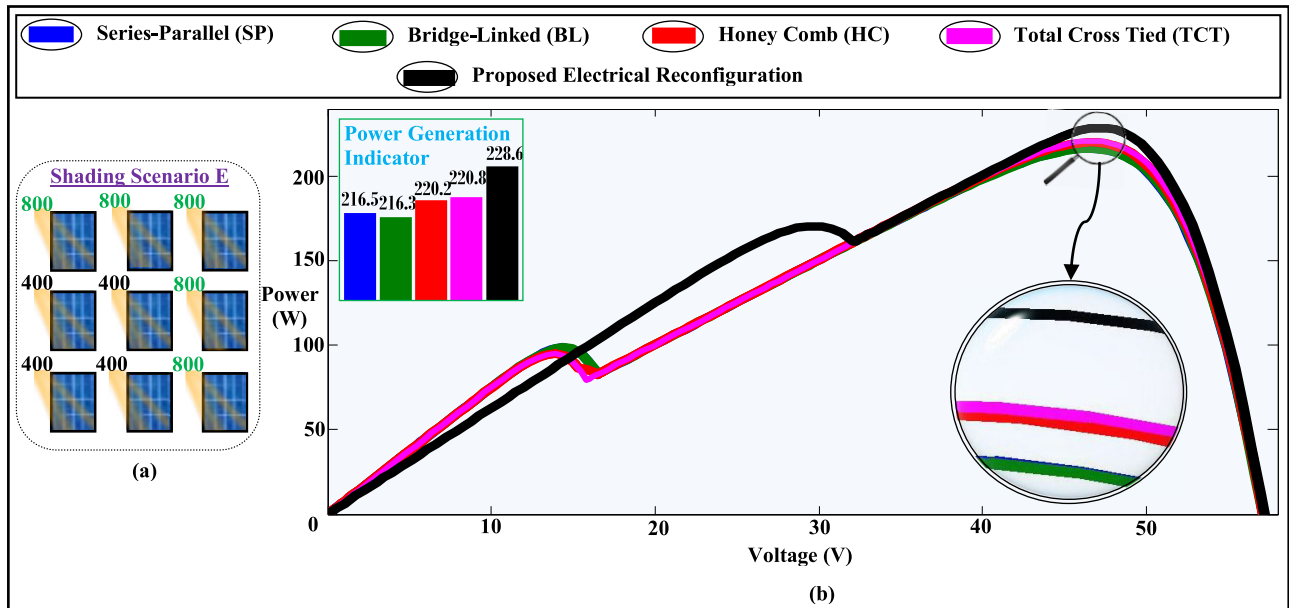
E. SCENARIO E
Scenario E is represented in FIGURE 18 (a) in which the first two modules of the second and third rows are receiving $400W/m^2$ whereas the other modules are operating under no shading scenario ($800W/m^2$). The power curves are depicted in FIGURE 18 (b) where it can be seen that the power generation of one-time electrical reconfiguration (230.57W) is higher followed by the TCT (220.83W), HC (220.20W), BL (216.28W) and SP (216.54W) array configurations. The

reconfigured PV array has the lowest losses of 87.04W (mismatch) and 48.75% (power) as compared to the SP (101.07W and 51.88%), BL (101.33W and 51.93%), HC (97.41W and 51.06%) and TCT (96.79W and 50.92%) configurations respectively. This leads to a higher power generation and conversion efficiencies in the case of array electrical reconfiguration of 10.81% and 91.38% as compared to the SP (10.16% and 85.82%), BL (10.14% and 85.71%), HC (10.33% and 87.27%) and TCT (10.36% and 87.51%) configurations. The performance ratios of SP, BL, HC, TCT and proposed reconfiguration have been calculated as 68.17%, 68.09%, 69.33%, 69.52% and 72.59% respectively. The power generation of the array with the proposed strategy is 6.47% higher than SP, 6.60% than BL, 4.70% than the HC and 4.41% than TCT configurations.

F. SCENARIO F
During scenario F (FIGURE 19 (a)), the PV modules present over the first and second rows of the array have been subjected to shading receiving lower irradiance levels of $100W/m^2$ whereas the modules of the third row received $800W/m^2$ (no shading). The total available power in the array under this shading is found as 128.76W. The power curves of the arrays have been shown in FIGURE 19 (b) representing that conventional configurations have equal power output

FIGURE 18. Partial shading scenario E for 3 × 3 PV array configurations and proposed reconfiguration. (a) Shading scenario, and (b) Power curves (simulation analysis).
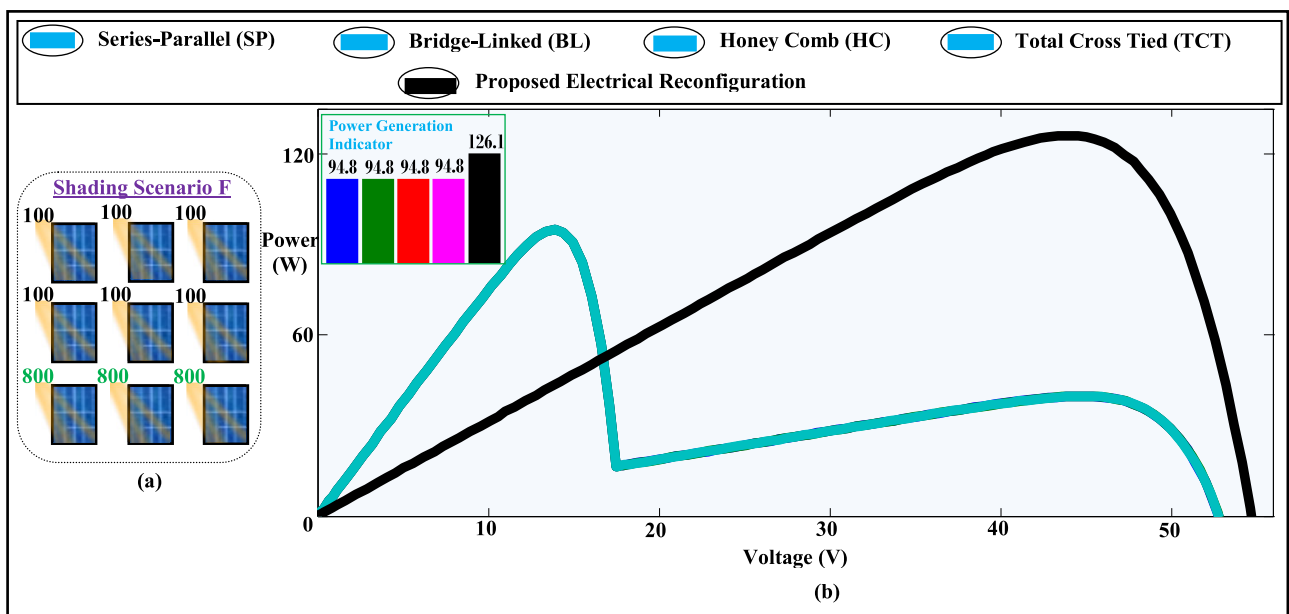

FIGURE 19. Partial shading scenario F for 3 × 3 PV array configurations and proposed reconfiguration. (a) Shading scenario, and (b) Power curves (simulation analysis).

i.e. 94.82W with mismatch loss of 222.79W, power loss of 78.92%, power generation efficiency of 4.44%, power conversion efficiency of 74% and performance ratio as 29.85%. However, the power output of one-time electrical reconfiguration is found to be higher i.e. 127.13W with lower losses of 189.48W (mismatch) and 71.52% (power). Also, there is a higher power output and conversion efficiencies of 6.01% and 98.75% respectively with a performance ratio of 40.02%. The

PV array with proposed reconfiguration has 34.07% power enhancement than the SP, BL, HC and TCT configurations.

The parameters comparison of the proposed technique with the SP, BL, HC and TCT configurations during all the above-studied scenarios has been graphically represented in FIGURE 20. The graphs clearly state that the proposed reconfiguration excelled in performance in terms of reduced losses and improved efficiencies during partial shading.
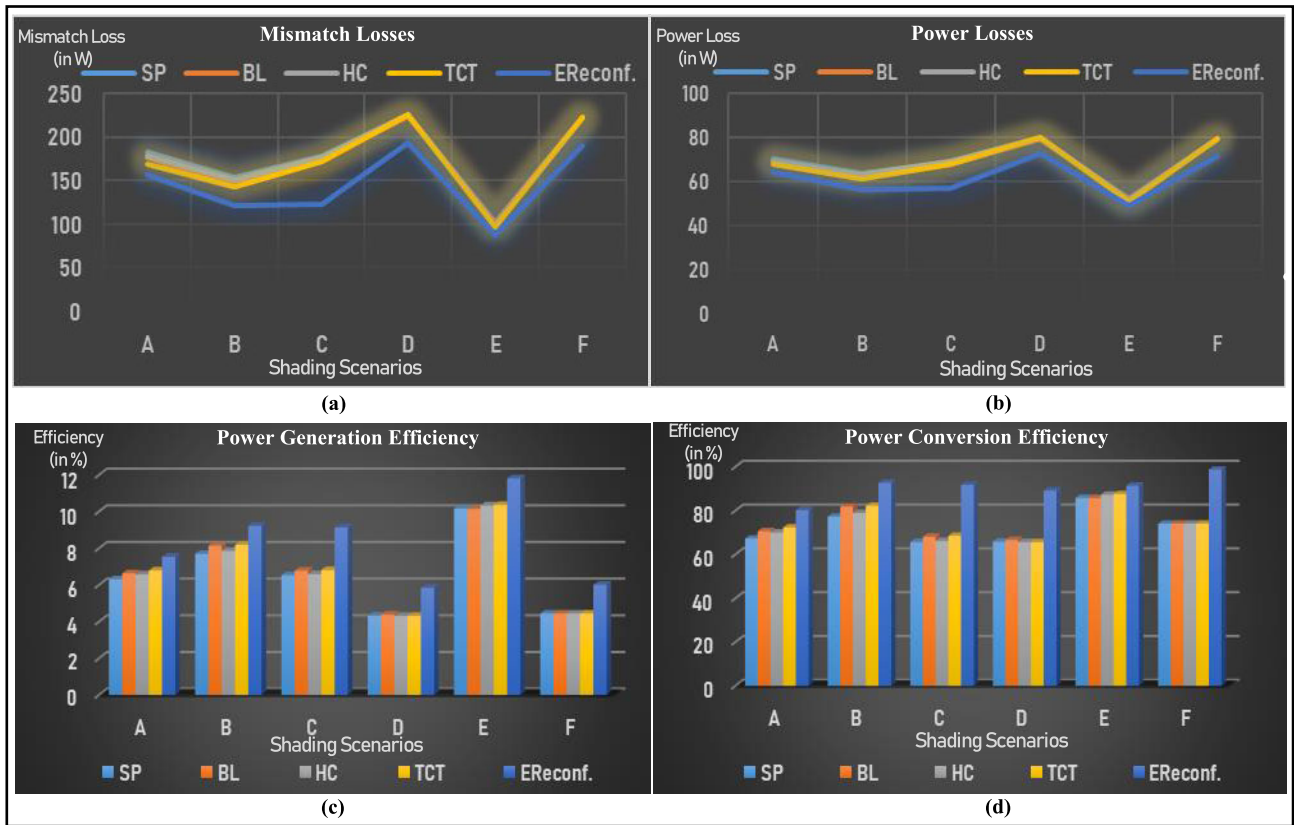
FIGURE 20. Graphical comparison of various performance parameters of 3 × 3 PV arrays with SP, BL, HC, TCT configurations and proposed one-time electrical reconfiguration. (a) Mismatch Losses, (b) Power Losses, (c) Power Generation Efficiency, and (d) Power Conversion Efficiency.

The comparative data obtained from the simulation and experiments for different 3×3 PV array configurations during shading scenarios A to F have been tabulated in Table 6. The results indicate that the array implemented with the proposed one-time electrical reconfiguration has shown excellent performance during all the shading scenarios.

Also, for enhanced analysis, several other partial shading scenarios for the 3 × 3 PV array have been considered. The shading scenarios, corresponding P-V characteristics curves and power generation of the conventional configurations and proposed electrical reconfiguration have been given in Table 7. The shading scenarios considered in the table replicate the possible occurrence in a real-time scenario due to the presence of the trees and buildings shadows. From the results given in Table 7, it can be observed that the electrical reconfiguration has significantly enhanced the power generation of the array during all the shading cases as compared to conventional configurations. Also, it has been observed that in some of the shading cases, the SP, BL, HC and TCT configurations have nearly equal power generations whereas there is a notable higher power output in the case of the proposed technique. Hence, it can be summarised from the results that the adoption of the proposed technique can significantly enhance the power generation of the 3 × 3 PV array during partial shading.

Similarly, to prove the efficacy of the proposed one-time electrical reconfiguration, a 9 × 9 array has been considered for investigation. The 9 × 9 array has been implemented with SP, BL, HC and TCT along with Sudoku reconfiguration and one-time electrical reconfiguration. The implementation of the Sudoku reconfiguration has been pictorially explained in FIGURE 4. The investigation has been carried out under three shading scenarios and compared with the SP, BL, HC, TCT and Sudoku reconfiguration.

During no shading scenario, the 9 × 9 PV arrays are operated at 800W/m^2 and 50°C generating the maximum power of 2858.57W whereas the shaded modules are operated at 100W/m^2. The shading case A for the 9 × 9 PV array configurations is shown in FIGURE 21 (a) and the shade dispersion by the Sudoku and proposed electrical reconfigurations are depicted in FIGURE 21 (b) and (c) respectively. The power curves of the TCT, Sudoku and one-time electrical reconfiguration are depicted in FIGURE 22.
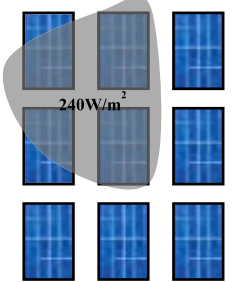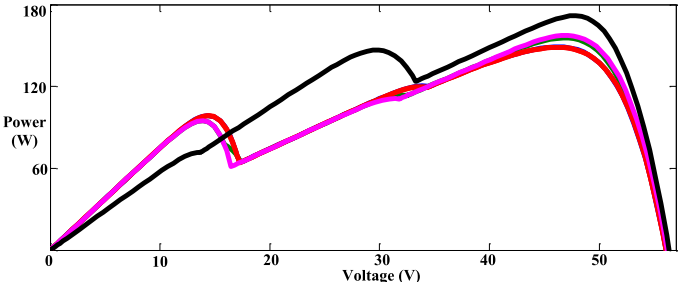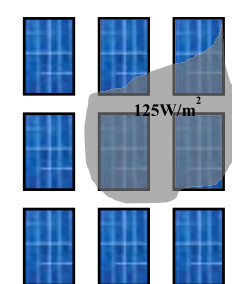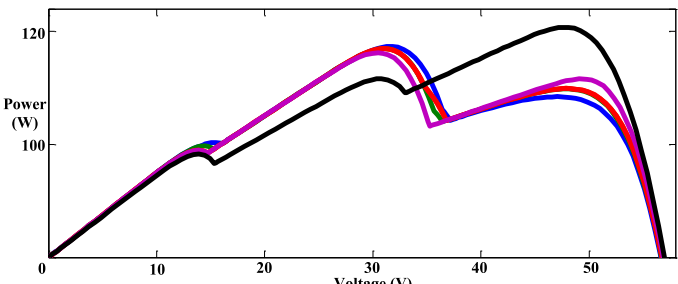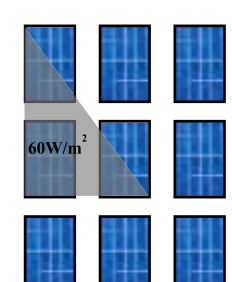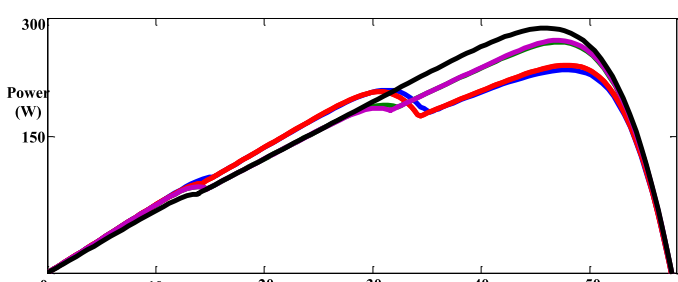
The maximum power output of SP, BL, HC, TCT, Sudoku and electrical reconfigurations during shading case A have been found as 2176.3W, 2439.2W, 2407.5W, 2553.6W, 2687.99W and 2719.68W respectively indicating higher power generation of the proposed one-time reconfiguration than others. The proposed technique has lower mismatch and power losses of 138.89W and 32.84% as compared to

TABLE 6. Simulation and experiments data of performance parameters of 3 × 3 configurations during various shading scenarios.

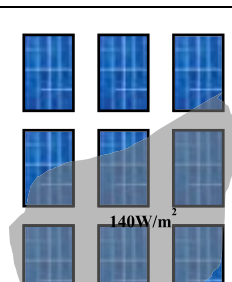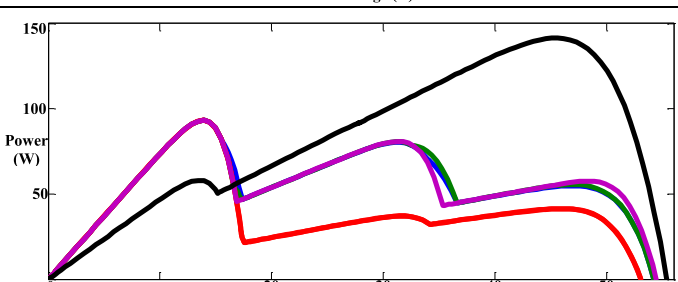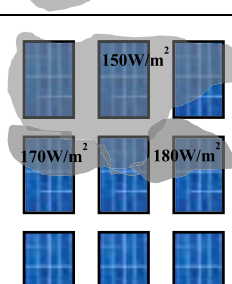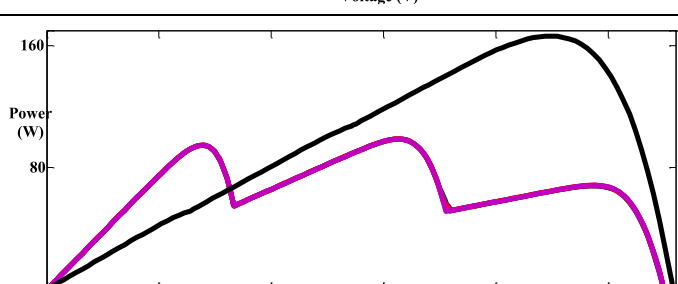| Shading Scenario A										
	Simulation Data					Experiments Data				
Performance Parameters	SP	BL	HC	TCT	E.Reconfg.	SP	BL	HC	TCT	E.Reconfg.
Available Power (W)			200.20					198.14		
Maximum Power (W)	134.55	141.32	140.15	144.71	160.61	132.86	139.72	138.72	142.71	158.76
Mismatch Losses (W)	183.06	176.29	177.46	167.9	157	183.55	176.69	177.69	173.70	157.65
Power Losses (%)	70.1	68.59	68.85	67.84	64.30	70.47	68.95	69.17	68.28	64.72
Generation Efficiency (%)	6.31	6.63	6.57	6.79	7.53	6.23	6.55	6.50	6.69	7.44
Conversion Efficiency (%)	67.20	70.58	70	72.29	80.22	67.05	70.51	70.01	72.02	80.12
Performance Ratio (%)	42.36	44.49	44.12	45.57	50.56	41.98	44.15	43.84	45.10	50.17
Shading Scenario B										
	Simulation Data					Experiments Data				
Performance Parameters	SP	BL	HC	TCT	E.Reconfg.	SP	BL	HC	TCT	E.Reconfg.
Available Power (W)			212.22					210.48		
Maximum Power (W)	163.89	173.59	167.53	174.37	196.66	162.03	171.55	165.56	172.39	194.60
Mismatch Losses (W)	153.72	144.02	150.08	143.24	120.95	154.38	144.86	150.85	144.02	121.81
Power Losses (%)	63.58	61.42	62.77	61.25	56.29	63.99	61.87	63.20	61.69	56.75
Generation Efficiency (%)	7.69	8.14	7.86	8.18	9.22	7.60	8.04	7.76	8.08	9.13
Conversion Efficiency (%)	77.22	81.79	78.94	82.16	92.66	76.98	81.50	78.65	81.90	92.45
Performance Ratio (%)	51.60	54.65	52.74	54.90	61.91	51.20	54.21	52.32	54.48	61.50
Shading Scenario C										
	Simulation Data					Experiments Data				
Performance Parameters	SP	BL	HC	TCT	E.Reconfg.	SP	BL	HC	TCT	E.Reconfg.
Available Power (W)			212.22					210.48		
Maximum Power (W)	141.20	146.42	143.35	147.40	196.65	139.35	144.50	140.59	145.30	194.66
Mismatch Losses (W)	178.26	173.11	177.12	172.31	122.95	177.06	171.91	175.82	171.11	121.75
Power Losses (%)	69.03	67.88	68.78	67.71	56.74	69.03	67.88	68.75	67.71	56.74
Generation Efficiency (%)	6.53	6.78	6.59	6.81	9.13	6.53	6.78	6.59	6.81	9.13
Conversion Efficiency (%)	65.66	68.08	66.20	68.46	91.72	66.20	68.65	66.79	69.03	92.48
Performance Ratio (%)	43.87	45.49	44.23	45.74	61.28	44.04	45.66	44.43	45.92	61.52
Shading Scenario D										
	Simulation Data					Experiments Data				
Performance Parameters	SP	BL	HC	TCT	E.Reconfg.	SP	BL	HC	TCT	E.Reconfg.
Available Power (W)			140.20					139.87		
Maximum Power (W)	92.27	93.35	92.06	91.98	124.99	93.45	94.23	93.16	92.63	124.97
Mismatch Losses (W)	225.34	224.26	225.55	225.63	192.62	222.96	222.18	223.25	223.78	191.44
Power Losses (%)	79.49	79.25	79.54	79.56	72.22	79.23	79.06	79.29	79.41	72.22
Generation Efficiency (%)	4.32	4.38	4.31	4.31	5.84	4.38	4.42	4.37	4.34	5.86
Conversion Efficiency (%)	65.81	66.58	65.66	65.58	89.15	66.81	67.36	66.60	66.22	89.34
Performance Ratio (%)	29.05	29.39	28.98	28.96	39.35	29.53	29.78	29.44	29.27	39.49
Shading Scenario E										
	Simulation Data					Experiments Data				
Performance Parameters	SP	BL	HC	TCT	E.Reconfg.	SP	BL	HC	TCT	E.Reconfg.
Available Power (W)			252.30					251.32		
Maximum Power (W)	216.54	216.28	220.20	220.82	230.57	225.89	225.81	221.67	222.15	231.94
Mismatch Losses (W)	101.07	101.33	97.41	96.79	87.04	90.52	90.6	94.74	94.26	84.47
Power Losses (%)	51.88	51.93	51.06	50.92	48.76	49.80	49.82	50.74	50.63	48.45
Generation Efficiency (%)	10.16	10.14	10.33	10.36	10.81	10.59	10.59	10.40	10.42	10.88
Conversion Efficiency (%)	85.82	85.71	87.27	87.51	91.38	89.88	89.84	88.20	88.39	92.28
Performance Ratio (%)	68.17	68.09	69.33	69.52	72.59	71.39	71.36	70.05	70.20	73.30
Shading Scenario F										
	Simulation Data					Experiments Data				
Performance Parameters	SP	BL	HC	TCT	E.Reconfg.	SP	BL	HC	TCT	E.Reconfg.
Available Power (W)			128.76					127.43		
Maximum Power (W)	94.82	94.82	94.82	94.82	127.13	95.52	95.64	95.58	95.67	126.89
Mismatch Losses (W)	222.79	222.79	222.79	222.79	222.79	220.89	220.77	220.83	220.74	186.52
Power Losses (%)	78.92	78.92	78.92	78.92	78.92	78.77	78.74	78.76	78.74	70.35
Generation Efficiency (%)	4.44	4.44	4.44	4.44	5.96	4.48	4.48	4.48	4.48	5.98
Conversion Efficiency (%)	73.64	73.64	73.64	73.64	98.73	74.95	75.05	75	75.07	99.57
Performance Ratio (%)	29.85	29.85	29.85	29.85	29.85	30.18	30.22	30.20	30.23	40.10

TABLE 7. Analysis of conventional configurations and electrical reconfiguration under additional shading scenarios for 3 × 3 PV arrays.

Shading Scenario	Corresponding P-V Curves	Power Generation
240W/m²		*Series-Parallel (SP)* **149.02W** *Bridge-Linked (BL)* **155.56W** *Honey Comb (HC)* **148.73W** *Total Cross Tied (TCT)* **157.35W** *Electrical Reconfiguration* **174.84W**
125W/m²		*Series-Parallel (SP)* **186.65W** *Bridge-Linked (BL)* **184.78W** *Honey Comb (HC)* **184.82W** *Total Cross Tied (TCT)* **181.09W** *Electrical Reconfiguration* **205.62W**
60W/m²		*Series-Parallel (SP)* **223.26W** *Bridge-Linked (BL)* **253.89W** *Honey Comb (HC)* **228.41W** *Total Cross Tied (TCT)* **255.68W** *Electrical Reconfiguration* **272.16W**
140W/m²		*Series-Parallel (SP)* **93.18W** *Bridge-Linked (BL)* **93.18W** *Honey Comb (HC)* **93.22W** *Total Cross Tied (TCT)* **93.18W** *Electrical Reconfiguration* **143.42W**
150W/m² 170W/m² 180W/m²		*Series-Parallel (SP)* **98.79W** *Bridge-Linked (BL)* **98.82W** *Honey Comb (HC)* **98.80W** *Total Cross Tied (TCT)* **98.76W** *Electrical Reconfiguration* **168.36W**

● Series-Parallel (SP)　● Bridge-Linked (BL)　● Honey Comb (HC)　● Total Cross Tied (TCT)　● Electrical Reconfiguration

TABLE 8. Performance summary of the proposed one-time electrical reconfiguration with SP, BL, HC, TCT and sudoku for 9 × 9 PV array.

Shading Case A						
Performance Parameters	**SP**	**BL**	**HC**	**TCT**	**Sudoku**	**One-time Reconfiguration**
Available Power (W)				2730.34		
Maximum Power (W)	2176.35	2436.97	2407.07	2553.62	2687.99	2719.68
Mismatch Losses (W)	686.22	421.60	451.50	304.95	170.58	138.89
Power Losses (%)	46.26	39.82	40.54	36.94	33.62	32.84
Generation Efficiency (%)	11.30	12.66	12.50	13.26	13.96	14.13
Conversion Efficiency (%)	79.70	89.25	88.16	93.52	98.44	99.60
Performance Ratio (%)	76.13	85.25	84.20	89.33	94.03	95.14
Shading Case B						
Performance Parameters	**SP**	**BL**	**HC**	**TCT**	**Sudoku**	**One-time Reconfiguration**
Available Power (W)				2478.9		
Maximum Power (W)	1991.38	2085.67	2084.18	2194.88	2406.62	2478.42
Mismatch Losses (W)	867.19	772.9	774.39	663.69	451.95	377.15
Power Losses (%)	50.83	48.50	48.53	45.80	40.57	38.73
Generation Efficiency (%)	10.34	10.83	10.82	11.40	12.50	12.89
Conversion Efficiency (%)	80.33	84.13	84.07	88.54	97.08	99.99
Performance Ratio (%)	69.66	72.96	72.90	76.78	84.18	86.70
Shading Case C (Diagonal Shading)						
Performance Parameters	**SP**	**BL**	**HC**	**TCT**	**Sudoku**	**One-time Reconfiguration**
Available Power (W)				2573.19		
Maximum Power (W)	2243.77	2525.24	2524.31	2568.02	2569.18	2572.39
Mismatch Losses (W)	614.8	333.33	334.26	290.55	142.39	56.38
Power Losses (%)	44.59	37.64	37.67	36.59	32.93	31.78
Generation Efficiency (%)	11.65	13.12	13.11	13.34	14.11	14.26
Conversion Efficiency (%)	87.19	98.13	98.10	99.79	99.81	99.99
Performance Ratio (%)	78.49	88.33	88.30	89.83	89.78	89.98
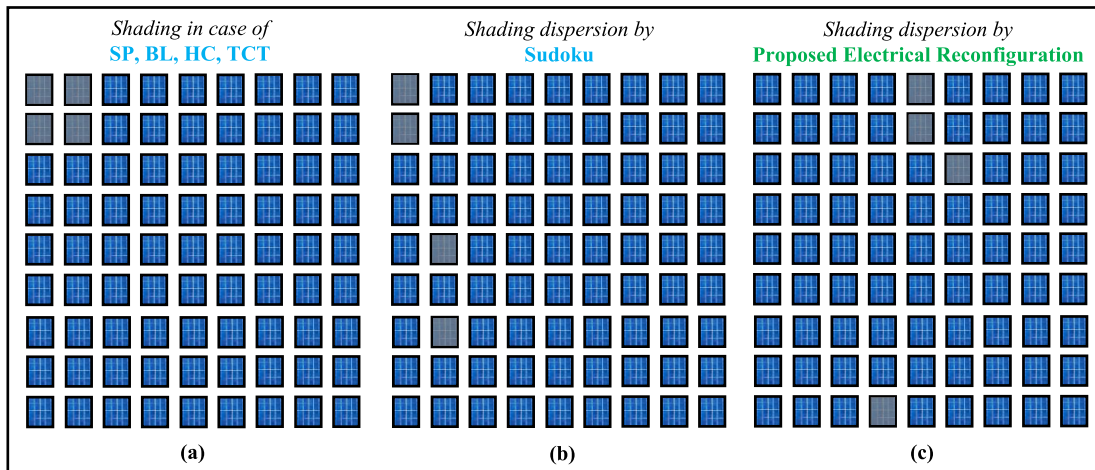
FIGURE 21. 9 × 9 array shading case A. (a) Shading in SP, BL, HC and TCT, (b) Shade dispersion by Sudoku reconfiguration, and (c) Shade dispersion by the proposed electrical reconfiguration.

the SP (686.22W and 46.26%), BL (421.60W and 39.82%), HC (451.50W and 40.54%), TCT (304.95W and 36.94%) and Sudoku (170.58W and 33.62%). The shading case B for the 9 × 9 array has been shown in FIGURE 23 (a) and the shade dispersion by the Sudoku and One-time electrical reconfigurations have been shown in FIGURE 23 (b) and (c) respectively. The power curves of the array with TCT, Sudoku and Electrical reconfiguration during shading case B have been depicted in FIGURE 24 representing that there is a significant power enhancement by the proposed strategy as compared to the Sudoku and other configurations. The

power output of the one-time electrical reconfiguration has been found as 2478.42W whereas the other configurations i.e. SP (1991.38W), BL (2986.7W), HC (2084.18W), TCT (2194.88W) and Sudoku (2406.62W) has the lowest power output. Similarly, the mismatch and power losses of the 9 × 9 PV array with electrical reconfiguration have been calculated as 5279.35W and 33.08% and found to be significantly lower as compared to the other configurations. The performance summary of the 9 × 9 PV array during shading case A, case B and shading case have been tabularized in Table 8.
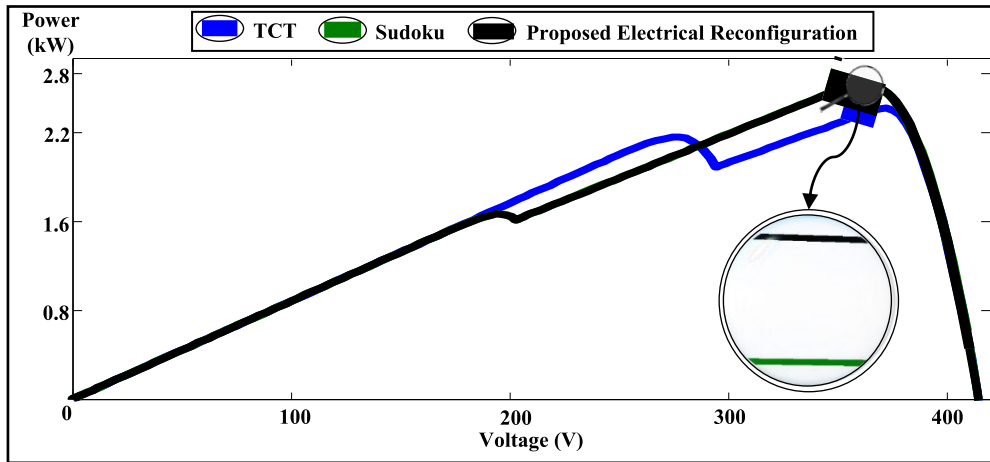
FIGURE 22. Power curves of 9 × 9 TCT, Sudoku and proposed One-time electrical Reconfiguration during shading case A (simulation analysis).
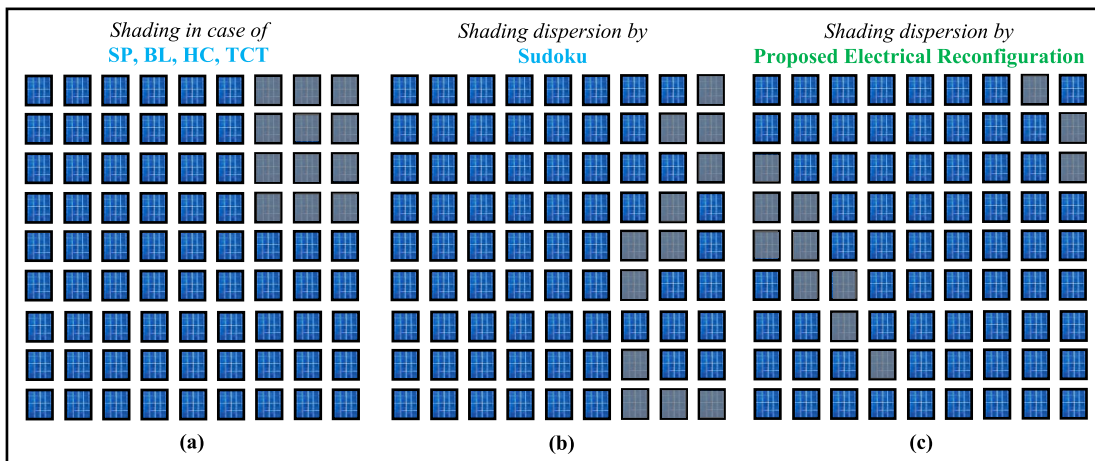

FIGURE 23. 9 × 9 array shading case B. (a) Shading in SP, BL, HC and TCT, (b) Shade dispersion by Sudoku reconfiguration, and (c) Shade dispersion by the proposed electrical reconfiguration.
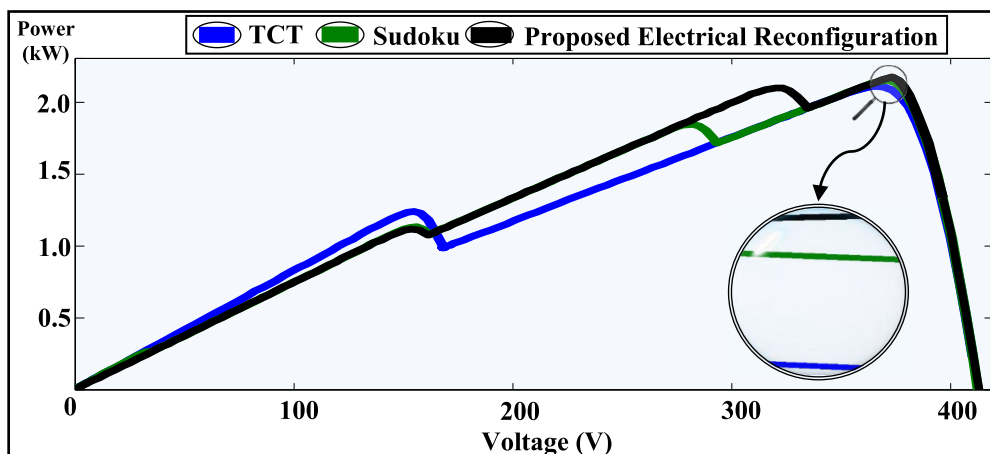
FIGURE 24. Power curves of 9 × 9 TCT, sudoku and proposed one-time electrical reconfiguration during shading case B (simulation analysis).

The above-conducted analysis gives clear evidence of the efficient functionality and shading mitigation ability of the one-time electrical reconfiguration in increasing the maximum power output and performance of the PV arrays. This results in a significant reduction in losses, improved efficiency and higher reliability of the array operating under

shading. The major merits of adopting the proposed strategy are:

- ➢ Higher power generation during shading
- ➢ Lowers the losses from the array
- ➢ Improved efficiency and performance during shading
- ➢ No physical repositioning of modules and hence, no manpower is required
- ➢ Ease of implementation in all types of PV systems
- ➢ Zero switches and sensors requirement
- ➢ No extra wire requirement (equivalent to TCT)
- ➢ Low cost and user-friendly.
- ➢ Ease fault diagnosis
- ➢ Effective shade mitigation
- ➢ Highly Reliable

Hence, the proposed strategy can be easily implemented in PV arrays as a cost-effective solution for reducing the power loss due to the presence of partial shading.

V. CONCLUSION

In this work, a one-time electrical reconfiguration for partial shading prone PV arrays has been proposed that can act as a fixed solution to reduce the losses from the arrays. The proposed reconfiguration has been tested for two PV array sizes (3×3 and 9×9) under different shading scenarios in MATLAB and real-time experimental environments. The investigation concludes that the proposed reconfiguration strategy has generated significantly higher power as compared to the series-parallel, bridge-linked, honeycomb, total cross tied and Sudoku reconfiguration. During partial shading. Also, the proposed strategy can efficiently reduce the losses and increase the overall efficiencies and performance of the PV arrays during partial shading as compared to other configurations. The average power enhancement of the proposed electrical reconfiguration during partial shading as compared to the series-parallel, bridge-linked, honeycomb and total-cross-tied configurations has been found as 25.84%, 22.69%, 23.66% and 21.69% respectively. Hence, the proposed electrical reconfiguration is a highly reliable solution for effective power enhancement and loss mitigation in PV arrays. The reconfiguration is easy to execute in partial shading prone PV arrays that require no modules position replacement, switches and sensors, extra wires and hence, no additional cost and complexities in the system.

REFERENCES

[1] D. Kaur and M. Rehman, "A literature review of understanding consumer behaviour in the adoption of solar energy products," *Solid State Technol.*, vol. 63, no. 6, pp. 11086–11101, 2020.

[2] D. P. Winston, S. Kumaravel, B. P. Kumar, and S. Devakirubakaran, "Performance improvement of solar PV array topologies during various partial shading conditions," *Sol. Energy*, vol. 196, pp. 228–242, Jan. 2020.

[3] O. Bingöl and B. Özkaya, "Analysis and comparison of different PV array configurations under partial shading conditions," *Sol. Energy*, vol. 160, pp. 336–343, Jan. 2018.

[4] C. G. Lee, W. G. Shin, J. R. Lim, G. H. Kang, Y. C. Ju, H. M. Hwang, H. S. Chang, and S. W. Ko, "Analysis of electrical and thermal characteristics of PV array under mismatching conditions caused by partial shading and short circuit failure of bypass diodes," *Energy*, vol. 218, Mar. 2021, Art. no. 119480.

[5] C. E. Clement, J. P. Singh, E. Birgersson, Y. Wang, and Y. S. Khoo, "Hotspot development and shading response of shingled PV modules," *Sol. Energy*, vol. 207, pp. 729–735, Sep. 2020.

[6] M. W. Akram, G. Li, Y. Jin, C. Zhu, A. Javaid, M. Z. Akram, and M. U. Khan, "Study of manufacturing and hotspot formation in cut cell and full cell PV modules," *Sol. Energy*, vol. 203, pp. 247–259, Jun. 2020.

[7] M. U. Ali, S. Saleem, H. Masood, K. D. Kallu, M. Masud, M. J. Alvi, and A. Zafar, "Early hotspot detection in photovoltaic modules using color image descriptors: An infrared thermography study," *Int. J. Energy Res.*, vol. 46, no. 2, pp. 774–785, Feb. 2022.

[8] K. A. K. Niazi, W. Akhtar, H. A. Khan, Y. Yang, and S. Athar, "Hotspot diagnosis for solar photovoltaic modules using a naive Bayes classifier," *Sol. Energy*, vol. 190, pp. 34–43, Sep. 2019.

[9] S. Daliento, F. Di Napoli, P. Guerriero, and V. d'Alessandro, "A modified bypass circuit for improved hot spot reliability of solar panels subject to partial shading," *Sol. Energy*, vol. 134, pp. 211–218, Sep. 2016.

[10] P. R. Satpathy, R. Sharma, S. K. Panigrahi, and S. Panda, "Bypass diodes configurations for mismatch and hotspot reduction in PV modules," in *Proc. Int. Conf. Comput. Intell. Smart Power Syst. Sustain. Energy (CISPSSE)*, Jul. 2020, pp. 1–6.

[11] P. R. Satpathy, T. S. Babu, A. Mahmoud, R. Sharma, and B. Nastasi, "A TCT-SC hybridized voltage equalizer for partial shading mitigation in PV arrays," *IEEE Trans. Sustain. Energy*, vol. 12, no. 4, pp. 2268–2281, Oct. 2021.

[12] K. Ishaque and Z. Salam, "A review of maximum power point tracking techniques of PV system for uniform insolation and partial shading condition," *Renew. Sustain. Energy Rev.*, vol. 19, pp. 475–488, Mar. 2013.

[13] J. Ahmed and Z. Salam, "A maximum power point tracking (MPPT) for PV system using cuckoo search with partial shading capability," *Appl. Energy*, vol. 119, pp. 118–130, Apr. 2014.

[14] H. Li, D. Yang, W. Su, J. Lü, and X. Yu, "An overall distribution particle swarm optimization MPPT algorithm for photovoltaic system under partial shading," *IEEE Trans. Ind. Electron.*, vol. 66, no. 1, pp. 265–275, Jan. 2019.

[15] M. Mansoor, A. F. Mirza, and Q. Ling, "Harris hawk optimization-based MPPT control for PV systems under partial shading conditions," *J. Cleaner Prod.*, vol. 274, Nov. 2020, Art. no. 122857.

[16] M. Mansoor, A. F. Mirza, Q. Ling, and M. Y. Javed, "Novel grass hopper optimization based MPPT of PV systems for complex partial shading conditions," *Sol. Energy*, vol. 198, pp. 499–518, Mar. 2020.

[17] M. N. I. Jamaludin, M. F. N. Tajuddin, J. Ahmed, A. Azmi, S. A. Azmi, N. H. Ghazali, T. S. Babu, and H. H. Alhelou, "An effective salp swarm based MPPT for photovoltaic systems under dynamic and partial shading conditions," *IEEE Access*, vol. 9, pp. 34570–34589, 2021.

[18] M. Joisher, D. Singh, S. Taheri, D. R. Espinoza-Trejo, E. Pouresmaeil, and H. Taheri, "A hybrid evolutionary-based MPPT for photovoltaic systems under partial shading conditions," *IEEE Access*, vol. 8, pp. 38481–38492, 2020.

[19] K. Guo, L. Cui, M. Mao, L. Zhou, and Q. Zhang, "An improved gray wolf optimizer MPPT algorithm for PV system with BFBIC converter under partial shading," *IEEE Access*, vol. 8, pp. 103476–103490, 2020.

[20] P. R. Satpathy and R. Sharma, "Reliability and losses investigation of photovoltaic power generators during partial shading," *Energy Convers. Manage.*, vol. 223, Nov. 2020, Art. no. 113480.

[21] P. R. Satpathy, S. Jena, and R. Sharma, "Power enhancement from partially shaded modules of solar PV arrays through various interconnections among modules," *Energy*, vol. 144, pp. 839–850, Feb. 2018.

[22] F. Belhachat and C. Larbes, "PV array reconfiguration techniques for maximum power optimization under partial shading conditions: A review," *Sol. Energy*, vol. 230, pp. 558–582, Dec. 2021.

[23] A. M. Ajmal, T. S. Babu, V. K. Ramachandaramurthy, D. Yousri, and J. B. Ekanayake, "Static and dynamic reconfiguration approaches for mitigation of partial shading influence in photovoltaic arrays," *Sustain. Energy Technol. Assessments*, vol. 40, Aug. 2020, Art. no. 100738.

[24] P. R. Satpathy, R. Sharma, and S. Jena, "A shade dispersion interconnection scheme for partially shaded modules in a solar PV array network," *Energy*, vol. 139, pp. 350–365, Nov. 2017.

[25] P. R. Satpathy and R. Sharma, "Power and mismatch losses mitigation by a fixed electrical reconfiguration technique for partially shaded photovoltaic arrays," *Energy Convers. Manage.*, vol. 192, pp. 52–70, Jul. 2019.

[26] B. Dhanalakshmi and N. Rajasekar, "Dominance square based array reconfiguration scheme for power loss reduction in solar Photo-Voltaic (PV) systems," *Energy Convers. Manage.*, vol. 156, pp. 84–102, Jan. 2018.

[27] S. Vijayalekshmy, G. R. Bindu, and S. R. Iyer, "A novel Zig-Zag scheme for power enhancement of partially shaded solar arrays," *Sol. Energy*, vol. 135, pp. 92–102, Oct. 2016.

[28] P. Satpathy, R. Sharma, and S. Dash, "An efficient sd-par technique for maximum power generation from modules of partially shaded pv arrays," *Energy*, vol. 175, pp. 182–194, 2019.

[29] P. R. Satpathy and R. Sharma, "Power loss reduction in partially shaded PV arrays by a static SDP technique," *Energy*, vol. 156, pp. 569–585, Aug. 2018.

[30] B. I. Rani, G. S. Ilango, and C. Nagamani, "Enhanced power generation from PV array under partial shading conditions by shade dispersion using Su Do Ku configuration," *IEEE Trans. Sustain. Energy*, vol. 4, no. 3, pp. 594–601, Jan. 2013.

[31] G. S. Krishna and T. Moger, "Improved SuDoKu reconfiguration technique for total-cross-tied PV array to enhance maximum power under partial shading conditions," *Renew. Sustain. Energy Rev.*, vol. 109, pp. 333–348, Jul. 2019.

[32] K. Rajani and T. Ramesh, "Maximum power enhancement under partial shadings using modified Sudoku reconfiguration," *CSEE J. Power Energy Syst.*, vol. 7, no. 6, pp. 1187–1201, Jul. 2020.

[33] S. N. Deshkar, S. B. Dhale, J. S. Mukherjee, T. S. Babu, and N. Rajasekar, "Solar PV array reconfiguration under partial shading conditions for maximum power extraction using genetic algorithm," *Renew. Sustain. Energy Rev.*, vol. 43, pp. 102–110, Mar. 2015.

[34] S. S. Reddy and C. Yammani, "A novel magic-square puzzle based one-time PV reconfiguration technique to mitigate mismatch power loss under various partial shading conditions," *Optik*, vol. 222, Nov. 2020, Art. no. 165289.

[35] T. S. Babu, D. Yousri, and K. Balasubramanian, "Photovoltaic array reconfiguration system for maximizing the harvested power using population-based algorithms," *IEEE Access*, vol. 8, pp. 109608–109624, 2020.

[36] A. M. Ajmal, V. K. Ramachandaramurthy, A. Naderipour, and J. B. Ekanayake, "Comparative analysis of two-step GA-based PV array reconfiguration technique and other reconfiguration techniques," *Energy Convers. Manage.*, vol. 230, Feb. 2021, Art. no. 113806.

[37] D. S. Pillai, N. Rajasekar, J. P. Ram, and V. K. Chinnaiyan, "Design and testing of two phase array reconfiguration procedure for maximizing power in solar PV systems under partial shade conditions (PSC)," *Energy Convers. Manage.*, vol. 178, pp. 92–110, Dec. 2018.

[38] T. S. Babu, J. P. Ram, T. Dragičević, M. Miyatake, F. Blaabjerg, and N. Rajasekar, "Particle swarm optimization based solar PV array reconfiguration of the maximum power extraction under partial shading conditions," *IEEE Trans. Sustain. Energy*, vol. 9, no. 1, pp. 74–85, Jan. 2018.

[39] D. Yousri, D. Allam, and M. B. Eteiba, "Optimal photovoltaic array reconfiguration for alleviating the partial shading influence based on a modified Harris hawks optimizer," *Energy Convers. Manage.*, vol. 206, Feb. 2020, Art. no. 112470.

[40] X. Zhang, C. Li, Z. Li, X. Yin, B. Yang, L. Gan, and T. Yu, "Optimal mileage-based PV array reconfiguration using swarm reinforcement learning," *Energy Convers. Manage.*, vol. 232, Mar. 2021, Art. no. 113892.

[41] H. Rezk, A. Fathy, and M. Aly, "A robust photovoltaic array reconfiguration strategy based on coyote optimization algorithm for enhancing the extracted power under partial shadow condition," *Energy Rep.*, vol. 7, pp. 109–124, Nov. 2021.

[42] A. Fathy, "Recent meta-heuristic grasshopper optimization algorithm for optimal reconfiguration of partially shaded PV array," *Sol. Energy*, vol. 171, pp. 638–651, Sep. 2018.

[43] H. Jeong, H. Lee, Y.-C. Liu, and K. A. Kim, "Review of differential power processing converter techniques for photovoltaic applications," *IEEE Trans. Energy Convers.*, vol. 34, no. 1, pp. 351–360, Mar. 2019.

[44] G. Chu, H. Wen, Y. Yang, and Y. Wang, "Elimination of photovoltaic mismatching with improved submodule differential power processing," *IEEE Trans. Ind. Electron.*, vol. 67, no. 4, pp. 2822–2833, Apr. 2020.

[45] G. Chu, H. Wen, Y. Hu, L. Jiang, Y. Yang, and Y. Wang, "Low-complexity power balancing point-based optimization for photovoltaic differential power processing," *IEEE Trans. Power Electron.*, vol. 35, no. 10, pp. 10306–10322, Oct. 2020.

PRIYA RANJAN SATPATHY received the B.Tech. degree in electrical engineering, the M.Tech. degree in renewable energy engineering and management, and the Ph.D. degree in solar photovoltaic power system (electrical engineering), in 2015, 2017, and 2022, respectively. He is currently a Research Associate with Department of Electrical and Electronics Engineering (EEE), Chaitanya Bharathi Institute of Technology (CBIT), Hyderabad, India. He was with the Council of Scientific and Industrial Research (CSIR), as a Senior Research Fellow, from 2021 to 2022. He has depth knowledge on different PV system softwares, including PVSyst, PVSOL, Sketchup, Helioscope, and AutoCAD. He has published two Indian patents and more than 40 papers in international journals and conferences till date. His research areas include solar power systems, PV array efficiency improvement and fault reduction, maximum power point tracking, and PV system design and installation (off-grid and on-grid). Also, he has been serving as a Reviewer for many international conferences and journals, such as IEEE, Elsevier, IET, Wiley, Springer, Frontiers, Taylor & Francis, and Hindawi, and reviewed more than 120 papers till date.

PRITAM BHOWMIK (Member, IEEE) received the M.Tech. and Ph.D. degrees in power system and power electronics from Siksha 'O' Anusandhan University, Bhubaneswar, India, in 2017 and 2021, respectively. He was with the Council of Scientific and Industrial Research (CSIR), Government of India, as a Senior Research Fellow, from 2019 to 2021. He is currently with the Department of Electrical Engineering, Budge Budge Institute of Technology, Kolkata, India, as an Associate Professor. He has authored or coauthored more than 20 of his research articles in international journals with high impact factors. His area of research interests include the topological study of microgrid, power sharing among static DGs in transient and steady state, study of the inertial response of microgrid and improvement, state of charge management, and study of V2G schemes.

THANIKANTI SUDHAKAR BABU (Senior Member, IEEE) received the B.Tech. degree from Jawaharlal Nehru Technological University, Anantapur, India, in 2009, the M.Tech. degree in power electronics and industrial drives from Anna University, Chennai, India, in 2011, and the Ph.D. degree from VIT University, Vellore, India, in 2017. He has completed his postdoctoral research fellowship in electrical power engineering with the Institute of Power Engineering, Universiti Tenaga Nasional (UNITEN), Malaysia. He is currently working as an Associate Professor with the Department of Electrical and Electronics Engineering, Chaitanya Bharathi Institute of Technology, Hyderabad, India. He has published more than 115 research articles in various renowned international journals. His research interests include design and implementation of solar PV systems, renewable energy resources, power management for hybrid energy systems, storage systems, fuel cell technologies, electric vehicle, and smart grid. He has been acting as an Editorial Board Member and a Reviewer for various reputed journals, such as IEEE Access, IEEE, IET, Elsevier, and Taylor & Francis.

CHIRANJIT SAIN (Member, IEEE) received the B.Tech. degree in electrical engineering from the Maulana Abul Kalam Azad University of Technology, Kolkata, India, the M.Tech. degree in mechatronics and automation (electrical engineering) from the National Institute of Technical Teachers Training and Research (NITTTR), Kolkata, India, and the Ph.D. degree in electrical engineering from the National Institute of Technology, Meghalaya, India, in 2019. He is currently an Assistant Professor with the Department of Electrical Engineering, Ghani Khan Choudhury Institute of Engineering & Technology, Malda, India. He is an Associate Member of the Institute of Engineers, India. His research interests include sensorless and vector control of permanent magnet motor drives, digital control in power electronics converters, electric vehicles, electrical machines design, and optimization and soft computing.

RENU SHARMA (Senior Member, IEEE) received the master's degree in electrical engineering from Jadavpur University, in 2006, and the Ph.D. degree in electrical engineering from SOA Deemed to be University, in 2014. She is currently working as a Professor and the Head of Department with the Department of Electrical Engineering, Siksha 'O' Anusandhan Deemed to be University, Bhubaneswar, India. She has published over 80 international journal and conference papers. Her research areas include smart grid, soft computing, solar photovoltaic systems, power system scheduling, evolutionary algorithms, and wireless sensor networks. She has over 20 years of leading impactful technical, professional, and educational experience. She is a Life Member of IE (India), a Member of IET, a Life Member of ISTE and ISSE, and the Chair of WIE IEEE Bhubaneswar Sub-Section. She was the General Chair of IEEE ODICON 2021, flagship conference IEEE WIECON-ECE 2020, Springer conference GTSCS-2020, and IEPCCT-2019. She is a Guest Editor of Special Issue on *International Journal of Power Electronics* and *International Journal of Innovative Computing and Applications* (Inderscience).

HASSAN HAES ALHELOU (Senior Member, IEEE) received the Ph.D. degree from the Isfahan University of Technology (IUT), Isfahan, Iran. He is currently a Faculty Member with Tisheen University, Lattakia, Syria. He has published more than 30 research papers in the high quality peer-reviewed journals and international conferences. He has also performed more than 160 reviews for high prestigious journals, including IEEE TRANSACTIONS ON INDUSTRIAL INFORMATICS, IEEE TRANSACTIONS ON INDUSTRIAL ELECTRONICS, *Energy Conversion and Management*, *Applied Energy*, and *International Journal of Electrical Power & Energy Systems*. He has participated in more than 15 industrial projects. His major research interests include power systems, power system dynamics, power system operation and control, dynamic state estimation, frequency control, smart grids, micro-grids, demand response, load shedding, and power system protection. He is included in the 2018 and 2019 Publons list of the top 1% best reviewer and researchers in the field of engineering. He was a recipient of the Outstanding Reviewer Award from *Energy Conversion and Management* journal, in 2016; *ISA Transactions* journal, in 2018; *Applied Energy* journal, in 2019; and many other awards. He was a recipient of the Best Young Researcher in the Arab Student Forum Creative among 61 researchers from 16 countries at Alexandria University, Egypt, in 2011.

⋯